

國立交通大學

環境工程研究所

碩士論文



考慮井部分貫穿效應之定水頭試驗
在非侷限含水層的解

**Laplace-domain solution for transient flow into a partially penetrating
well in unconfined aquifers under the constant-head test**

研究生：陳庚轅
指導教授：葉弘德

中華民國九十九年八月

考慮井部分貫穿效應之定水頭試驗在非侷限含水層的解

**Laplace-domain solution for transient flow into a partially penetrating
well in unconfined aquifers under the constant-head test**

研究生：陳庚轅
指導教授：葉弘德

Student: Geng-Yuan Chen
Advisor: Hund-Der Yeh

國立交通大學



Submitted to Institute of Environmental Engineering
College of Engineering
National Chiao Tung University
in partial Fulfillment of the Requirements
for the Degree of
Master of Science
in Environmental Engineering

August 2010

Hsinchu, Taiwan

中華民國九十九年八月


考慮井部分貫穿效應之定水頭試驗在非侷限含水層的解

研究生：陳庚轅

指導教授：葉弘德

國立交通大學環境工程研究所

摘 要



進行定水頭試驗時，需在抽水井中維持固定的水位高，並同時測量觀測井內洩降隨時間的變化。本研究考慮在非侷限含水層裡有一部分貫穿井作定水頭試驗，推導水層水位分佈之半解析解。本研究首先將部分貫穿井濾管部分設為定水頭邊界、盲管部分設為不透水邊界，接著以自由液面條件來描述非侷限含水層的上邊界，最後利用分離變數法及拉普拉斯轉換，推導得半解析解。此解可用來產生無因次洩降與時間之關係曲線，探討部分貫穿井在水層中所造成的垂直流問題，亦可利用試驗數據來推求水層的參數。

關鍵詞：地下水，非侷限含水層，部分貫穿，定水頭試驗

Laplace-domain solution for transient flow into a partially penetrating well in unconfined aquifers under the constant-head test

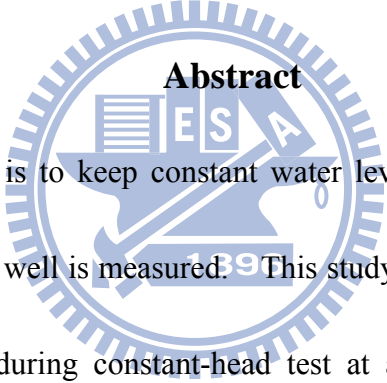
Student:Geng-Yuan Chen

Advisor:Hund-Der Yeh

Institute of Environmental Engineering

National Chiao Tung University

Abstract

The logo of the Water Resources Engineering Society (WRES) is a circular emblem with a gear-like border. Inside the circle, there is a stylized figure of a person holding a water tap, with the letters 'WRES' and the year '1991' integrated into the design.

The constant head test is to keep constant water level in the pumping well while the drawdown into the observed well is measured. This study derives a semi-analytical solution for drawdown distribution during constant-head test at a partially penetrating well in an unconfined aquifer. The constant-head condition is used to describe the boundary along the screen while no-flow condition is employed to describe the boundary along the casing of the well. In addition, a free surface condition is utilized to delineate the upper boundary of the unconfined aquifer. The Laplace domain solution is then derived using separation of variables and Laplace transform. This solution can be used to produce the curves of dimensionless drawdown versus dimensionless time to investigate the effects of vertical-flow caused by the partially penetration well and free surface boundary in an unconfined aquifer or

to identify the aquifer parameters from the data of constant-head test.

Keywords: Groundwater, Unconfined aquifer, partially penetrating well, constant-head test.



誌謝

首先誠摯的感謝指導教授葉弘德，老師悉心的教導使我得以一窺地下水領域的深奧，不時的討論並指點我正確的方向，使我在這兩年中獲益匪淺。老師對學問的嚴謹更是我輩學習的典範。本論文的完成另外亦得感謝口試委員台灣大學劉振宇教授、中國科技大學陳主惠教授、及中興大學謝平城教授有你們的指正及建議，使得本論文能夠更完整而嚴謹。

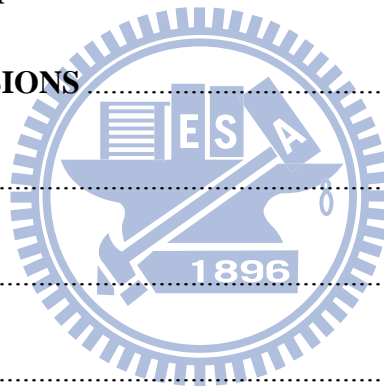
除了老師外，最感謝的就是雅琪與彥如學姊，不厭其煩的指出我研究中的缺失，且總能在我迷惘時為我解惑。感謝智澤、彥禎、玉德、仲豪、玳儀學長、敏筠、其珊學姐、國豪、玉霖、昭志學弟們，兩年裏的日子，實驗室裏共同的生活點滴，學術上的討論，感謝眾位學長姐、同學、學弟妹的共同砥礪，你們的陪伴讓兩年的研究生活變得絢麗多彩。也感謝璟勝，課業的討論和有著趕作業的革命情感。士賓和博傑學長壘球的啟發，信元、展帆、金澄、阿嚕、家馨、恰恰……排球隊一起運動和比賽，當然還有摯友勝然和信佑從大學到研究所就一起鼓勵與支持，恭喜我們順利走過這兩年。女朋友怡蓁在背後的默默支持更是我前進的動力，沒有怡蓁的體諒、包容，相信這兩年的生活將是很不一樣的光景。

最後，將本論文獻給我最親愛的雙親，冠億，鶴升你們是我最親愛的家人，給我有形與無形的支柱，謹將這份成果與榮耀與你們分享。

Table of Contents

中文摘要	I
Abstract	II
誌謝	IV
Table of Contents	V
LIST OF FIGURES	VII
NOTATION	VIII
CHAPTER 1 INTRODUCTION	1
1.1 Background	1
1.2 Literature Review	2
1.3 Objectives	6
CHAPTER 2 MATHEMATICAL DERIVATIONS	7
2.1 Mathematical Model of Constant-Head pumping Test	7
2.1.1 Governing Equations	7
2.1.2 Initial and boundary conditions	8
2.2 Laplace-domain solution	10
2.3 Fully penetrating wells in unconfined and confined aquifers	12
CHAPTER 3 NUMERICAL EVALUATION	13
3.1 Shanks Method	13
3.2 Numerical Inversion	14

CHAPTER 4 RESULTS AND DISCUSSION	16
4.1 Effective distance for the observation well with different specific time	16
4.2 Influence of specific yield	16
4.3 Effect of screen length	17
4.4 Effective distance for the observation well	17
4.5 Effect of anisotropy	18
4.6 Influence of the well radius	19
4.7 Effect of partially penetration	19
CHAPTER 5 CONCLUSIONS	20
APPENDIX A	21
APPENDIX B	29
APPENDIX C	33
REFERENCES	36



LIST OF FIGURES

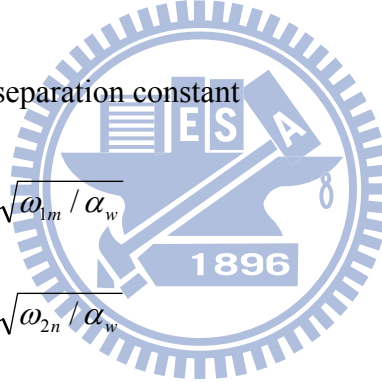
Fig 1. Schematic representation of an unconfined aquifer with a partially penetrating well...	41
Fig 2. The dimensionless drawdown distributions at $\tau =$ (a) 1 , (b) 10^2 , (c) 10^4 , and (d) 10^6	42
Fig 3. The effect of specific yield on the dimensionless drawdown during CHT.	43
Fig 4. The dimensionless drawdown distributions at the well screen extended from $\zeta = \zeta_l$ to $\zeta = \beta$ in region 2.	44
Fig 5. Relationship for dimensionless drawdown versus dimensionless time with $\zeta = 50 , 75$, and 100 at $\rho = 10$ or 100 for $S_y =$ (a) 0 and (b) 0.1.....	45
Fig 6. Spatial flow pattern in an unconfined aquifer with a partially penetrating well for $\kappa = 1$, $\beta = 100$, $\zeta_l = 25$, $S = 10^{-4}$ at $\tau = 10^4$ when $S_y =$ (a) 0 and (b) 0.1.....	46
Fig 7. The effect of conductivity ratio (κ) of region 2 on the dimensionless drawdown during CHT.	47
Fig 8. Drawdown distribution for a well with three different well radii ($r_w = 1, 0.1$ and 0.01 m) with $\sigma = 10^3$, $\zeta = 0.75$, $\zeta_l = 0.5$ and $\kappa = 1$	48
Fig 9. Effect of α on drawdown in a 100 m thick aquifer when $\sigma = 10^3$, $\kappa = 1$ at $\zeta = 0$ and $r = 100, 31.62$, and 10 m for $\alpha = 10^0, 10^{-1}$ and 10^{-2} , respectively.	49

NOTATION

A_{1m}'	$A_{1m}(p)I_0(\sqrt{p + \omega_{1m}})$
A_{2n}'	$A_{2n}(p)K_0(\sqrt{p + \omega_{2n}})$
b	Initial saturated thickness
h_0	Initial head
h	Hydraulic head
$I_0(\cdot)$	modified Bessel functions of the first kinds of order zero
$I_1(\cdot)$	modified Bessel functions of the first kinds of order one
i_{0m}	$I_0(\sqrt{p + \omega_{1m}}) / (\sqrt{p + \omega_{1m}} \cdot I_1(\sqrt{p + \omega_{1m}}))$
$K_0(\cdot)$	modified Bessel functions of the second kinds of order zero
$K_1(\cdot)$	modified Bessel functions of the second kinds of order one
K_r	Radial hydraulic conductivity
K_z	Vertical hydraulic conductivity
k_{0n}	$(\sqrt{p + \omega_{2n}} \cdot K_1(\sqrt{p + \omega_{2n}})) / K_0(\sqrt{p + \omega_{2n}})$
P	Laplace variable

r	Radial distance from the centerline of the well
r_w	Well radius
s_1^*	s_1 / s_w , dimensionless drawdown in region 1
s_2^*	s_2 / s_w , dimensionless drawdown in region 2
$\tilde{s}_1^*(\rho, \zeta, P)$	dimensionless drawdown in Laplace domain for region 1
$\tilde{s}_2^*(\rho, \zeta, P)$	dimensionless drawdown in Laplace domain for region 2
S_s	Specific storage
s_w	Constant drawdown in the well
S_y	Specific yield
t	Time from the start of test
z	Vertical distance from the bottom of the aquifer
z_l	Lower z coordinate of well screen
α	$\alpha = \alpha_w \rho^2$
α_w	$\alpha_w = \kappa \rho_w^2$
β	b / r_w
ζ	z / b

ζ_l	z_l / b
η	saturated thickness
ρ	$\rho = r / r_w$
ρ_w	$\rho_w = r_w / b$
σ	$\sigma = S_y / S_s b$
τ	$K_r t / S_s r_w^2$, dimensionless time
ω_{1m}	separation constant
ω_{1n}	separation constant
Ω_1	$\sqrt{\omega_{1m} / \alpha_w}$
Ω_2	$\sqrt{\omega_{2n} / \alpha_w}$



CHAPTER 1 INTRODUCTION

1.1 Background

Groundwater is water stored in aquifers. A unit of rock or an unconsolidated deposit is called an aquifer when it can yield a usable quantity of water. There are two common types of aquifers: confined and unconfined. Confined aquifer includes upper and lower confining beds which are of low permeability. Unconfined aquifers are sometimes also called water table aquifers, because their upper boundary is a water table.

There are two main hydraulic parameters play a crucial role for the aquifer system in response to the test: transmissivity and storativity. Transmissivity describes the ease with which water can move through an aquifer and is a product of hydraulic conductivity and aquifer thickness. The behavior of hydraulic conductivity is similar to transmissivity. Hydraulic conductivity has the same unit as velocity. Storativity is defined as the dimensionless volume of water that an aquifer releases.

Two types of tests, named constant-head test (CHT) and constant-flux test (CFT), are usually performed to characterize an aquifer for estimating the hydraulic parameters. The CHT is usually employed for low-transmissivity aquifers, i.e., for aquifers with clay and/or silt formation. The drawdown/buildup should be kept at a constant value during the test period. On the other hand, the CFT is commonly used for high-transmissivity aquifers

which are mainly composed of sand and/or gravel materials. The well discharge rate should be kept at a constant value during the pumping period.

1.2 Literature Review

For aquifers with low-transmissivity, CHT is more suitable to apply than CFT. The wellbore storage at the pumping well has large effect on the early time drawdown behavior at pumping and observation wells in CFT (Renard, 2005). If a CHT is established in a short period of time, the effect of wellbore storage is negligible under the situations that the aquifer has low transmissivity and the well radius is small (Chen and Chang, 2003).

In the past, many studies had been devoted to the solutions for CHT. Kirkham (1959) derived a steady-state solution for groundwater distribution in a bounded confined aquifer pumped by a partially penetrating well under CHT. They simplified the complexity of the geometry by dividing the model into two different regions. Javandel and Zaghi (1975) considered the groundwater in a confined aquifer pumped by a fully penetrating well that is radially extended at the bottom of the aquifer. The procedure used in their study is similar to that in Kirkham (1959) and the steady-state groundwater solution was obtained using separation of variables. Jones et al. (1992) and Jones (1993) discussed the practicality of CHTs on wells completed in low-conductivity glacial till deposits. Mishra and Guyonnet (1992) indicated the operational benefit of CHTs in situations where the total available

drawdown is limited by well construction and aquifer characteristics. They developed a method for analyzing observation well response under a CHT. There have been numerous studies in the literature using CHT [e.g., Wilkinson, 1968; Uraiet and Raghaven, 1980; Hiller and Levy, 1994; Chen and Chang, 2003; Singh, 2007].

Considering a CHT performed in a partially penetrating well, Yang and Yeh (2005) developed a time-domain solution to describe the drawdown in a confined aquifer with finite thickness skin. The boundary conditions along the partially penetrating well are represented by a constant-head (first kind) boundary for the screen while a no-flow (second kind) boundary for the casing. They transformed the first kind boundary along the screen into a second kind boundary with an unknown flux which is time-dependent and therefore the boundary along the partially penetrating well became uniform. The solution was then solved by the Laplace and finite Fourier cosine transforms. Chang and Yeh (2009) used the methods of dual series equations and perturbation method to solve the mixed boundary problem for the CHT at a partially penetrating well. Chang and Yeh (2010) developed a new model describing a CHT performed in flowing partially penetrating well for arbitrary location of the well screen in a finite thick aquifer in depth. However, the studies mentioned above are only applicable for confined aquifers.

For unconfined aquifers, Chen and Chang (2003) developed a well hydraulic theory for CHT performed in a fully penetrating well and established a parameter estimation method.

Chang et al. (2010) extended the work of Yang and Yeh (2005) to develop a mathematical model for an unconfined aquifer system while treating the skin as a finite thickness zone and derived the associated solution for CHT at a partially penetrating well. For other environmental applications, light nonaqueous phase liquids (LNAPLs) are usually recovered by wells held at constant drawdown (Abdul, 1992; Murdoch and Franco, 1994) and a constant-head pumping is employed to control off-site migration of contaminated groundwater (Hiller and Levy, 1994). At LNAPL contaminant sites the pollutant forms a pool of LNAPL in the subsurface on the top of water table. It is therefore to install a well with the screen goes from the top of the aquifer in unconfined aquifers.

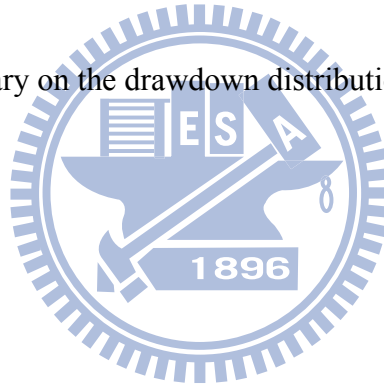
For the research of CFT in unconfined aquifers, Neuman (1972) presented a new analytical solution for characterizing flow to a fully penetrating well in an unconfined aquifer. He assumed the drainage above the water table occurs instantaneously. Take into account the effect of finite diameter pumping well, Moench (1997) developed a solution in Laplace-domain for the flow to a partially penetrating well in unconfined aquifers. Contrary to Neuman's assumption, he used the free-surface boundary in Boulton (1954) under the assumption that the drainage of pores occurs as an exponential function of time in response to a step change in hydraulic head in the aquifer. Tartakovsky and Neuman (2007) presented an analytical solution for drawdown in an unconfined aquifer due to pumping at a constant rate from a partially penetrating well. They generalized the solution of Neuman (1972, 1974)

by accounting for unsaturated flow above the water table and derived the solution from a linearized Richards' equation in which unsaturated hydraulic conductivity and water content are expressed as exponential functions of incremental capillary pressure head relative to its air entry value. Malama et al. (2007) utilized Laplace and Hankel transforms to obtain a semi-analytical solution for the problem of flow with leakage in an unconfined aquifer bounded below by an aquitard of finite or semi-infinite vertical extent. Malama et al. (2008) further extended their previous work to a system consisting of unconfined and confined aquifers, separated by an aquitard. The unconfined aquifer is pumped at a constant rate from a partially penetrating well. Pasadi et al. (2008) considered the effect of wellbore storage and finite-thickness skin and presented a Laplace-domain solution for CFT conducted in an unconfined aquifer with a partially penetrating well.

More recently, Malama et al. (2009a) developed a semi-analytic solution for a three-layered system, consisting of an aquifer and two confining units, due to constant rate pumping of the aquifer at a fully penetrating well. Their solution was successfully tested on the streaming potential data presented by Rizzo et al. (2004). Malama et al. (2009b) also developed a semi-analytic solution for a fully penetrating well in an unconfined aquifer under constant-rate pumping. Their solution was applied to estimate aquifer parameters using data recorded at the Boise Hydrogeophysical Research Site.

1.3 Objectives

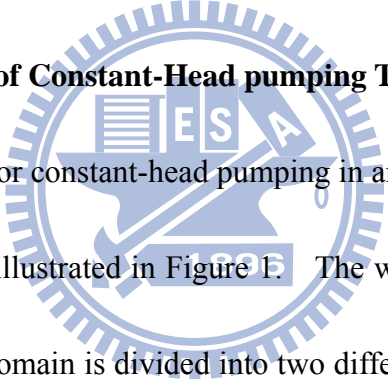
Motivated by the literatures above, the purpose of this paper is to develop a mathematical model for describing the drawdown distribution in an unconfined aquifer when performing the constant-head test in a partially penetrating well. Without assuming constant-head boundary along the screen as an unknown flux boundary, the system is separated into two different regions and the solution of the model is directly obtained using method of separation of variables and Laplace transform. This new solution can be used to determine the aquifer parameters or to investigate the effects of vertical-flow caused by the partially penetration well and free surface boundary on the drawdown distribution in unconfined aquifers.



CHAPTER 2 MATHEMATICAL DERIVATIONS

This chapter is divided into three parts. First, we develop a mathematical model for describing the drawdown distribution due to the pumping from a partially penetrating well in unconfined aquifers under constant-head test. The solution of the model is then derived by Laplace transforms. Final, the Laplace-domain solution can be shown to reduce to the solution in the case with a fully penetrating well.

2.1 Mathematical Model of Constant-Head pumping Test

The logo of the Water Resources Institute is a circular emblem with a gear-like border. Inside the circle, there is a stylized map of India. Overlaid on the map are the letters 'E', 'S', and 'A' in a grid-like arrangement. Below the map, the year '1925' is inscribed. The entire logo is rendered in a light blue color.

The conceptual model for constant-head pumping in an unconfined aquifer system with a partially penetrating well is illustrated in Figure 1. The well screen starts from $z = z_l$ with a finite well radius r_w . The domain is divided into two different regions. Region 1 is defined by $0 \leq r \leq r_w$ and $0 \leq z \leq z_l$ while region 2 is bounded within $r_w \leq r < \infty$ and $0 \leq z \leq \eta$ where η is the saturated thickness.

2.1.1 Governing Equations

The aquifer is assumed to be homogeneous, infinite extent in the radial direction and the seepage face in region 2 is neglected. The governing equations in terms of drawdown in the regions 1 and 2 can, respectively, be written as:

$$K_r \left(\frac{\partial^2 s_1}{\partial r^2} + \frac{1}{r} \frac{\partial s_1}{\partial r} \right) + K_z \frac{\partial^2 s_1}{\partial z^2} = S_s \frac{\partial s_1}{\partial t}, \quad 0 \leq r \leq r_w, \quad 0 \leq z \leq z_l \quad (1)$$

and

$$K_r \left(\frac{\partial^2 s_2}{\partial r^2} + \frac{1}{r} \frac{\partial s_2}{\partial r} \right) + K_z \frac{\partial^2 s_2}{\partial z^2} = S_s \frac{\partial s_2}{\partial t}, \quad r_w \leq r < \infty, \quad 0 \leq z \leq \eta \quad (2)$$

The subscripts 1 and 2 denote the regions 1 and 2, respectively. The drawdown at a distance r from the center of the well and a distance z from the bottom of the aquifer at time t is denoted as $s(r, z, t)$ which is equal to $h_0 - h$, where h_0 is the initial head and h is the hydraulic head. The aquifer has the horizontal hydraulic conductivity K_r , vertical hydraulic conductivity K_z , and specific storage S_s . Assume the drawdown is small in comparison with the saturated aquifer thickness η , the boundary at the free surface ($z = \eta$) can be approximated as $z = b$, where b is the initial saturated thickness. Therefore, the governing equation for region 2 can be further expressed as

$$K_r \left(\frac{\partial^2 s_2}{\partial r^2} + \frac{1}{r} \frac{\partial s_2}{\partial r} \right) + K_z \frac{\partial^2 s_2}{\partial z^2} = S_s \frac{\partial s_2}{\partial t}, \quad r_w \leq r < \infty, \quad 0 \leq z \leq b \quad (3)$$

2.1.2 Initial and boundary conditions

The initial condition for saturated thickness $\eta(r, t)$ is equal to b , the drawdowns are therefore assumed to be zero initially in regions 1 and 2, that is

$$s_1(r, z, 0) = s_2(r, z, 0) = 0 \quad (4)$$

The no-flow boundary condition at the bottom of the aquifer for both regions is

$$\left. \frac{\partial s_1(r, z, t)}{\partial z} \right|_{z=0} = \left. \frac{\partial s_2(r, z, t)}{\partial z} \right|_{z=0} = 0 \quad (5)$$

The bottom of the well screen ($z = z_l$) is assumed to be sealed and the boundary condition for s_1 at this position is therefore a no-flow boundary. It is thus expressed as

$$\left. \frac{\partial s_1(r, z, t)}{\partial z} \right|_{z=z_l} = 0, \quad 0 < r \leq r_w \quad (6)$$

The three-dimensional equation describing the flow at free surface for the unconfined aquifer can be written as (Batu, 1998, p.107)

$$K_x \left(\frac{\partial h}{\partial x} \right)^2 + K_y \left(\frac{\partial h}{\partial y} \right)^2 + K_z \left(\frac{\partial h}{\partial z} \right)^2 - K_z \frac{\partial h}{\partial z} = S_y \frac{\partial h}{\partial t} \quad \text{at} \quad z = b \quad (7)$$

where S_y is the specific yield.

Considering the drainage process is transient and the drawdown everywhere of the system is small in comparison to initial saturated thickness b . Using the linearized form that neglecting the second-order terms of the hydraulic gradient in Eq. (7) of the kinematic boundary condition at the water table (Neuman, 1972), the condition for the top boundary of the region 2 is

$$K_z \left. \frac{\partial s_2(r, z, t)}{\partial z} \right|_{z=b} = -S_y \left. \frac{\partial s_2(r, z, t)}{\partial t} \right|_{z=b}, \quad r_w \leq r < \infty \quad (8)$$

In addition, the boundary at $r = 0$ due to symmetry along the center of the well is written as:

$$\left. \frac{\partial s_1(r, z, t)}{\partial r} \right|_{r=0} = 0, \quad 0 < z < z_l \quad (9)$$

When r approaches infinity, the influence radius does not significantly affect the drawdown (Batu, 1998). The remote boundary is therefore taken at ∞ instead of the influence radius.

The boundary condition for the region 2 is

$$s_2(\infty, z, t) = 0 \quad (10)$$

The boundary condition specified along the well is

$$s_2(r_w, z, t) = s_w, \quad z_l < z < b, \quad t > 0 \quad (11)$$

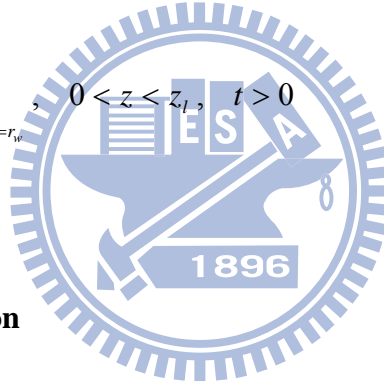
where s_w is a constant drawdown in the well at any time.

At the interface between regions 1 and 2, the continuities of the drawdown and flow rate must be satisfied:

$$s_1(r_w, z, t) = s_2(r_w, z, t), \quad 0 < z < z_l, \quad t > 0 \quad (12)$$

and

$$\left. \frac{\partial s_1(r, z, t)}{\partial r} \right|_{r=r_w} = \left. \frac{\partial s_2(r, z, t)}{\partial r} \right|_{r=r_w}, \quad 0 < z < z_l, \quad t > 0 \quad (13)$$



2.2 Laplace-domain solution

In order to express the solutions in dimensionless form, following dimensionless variables are defined: $s_1^* = s_1 / s_w$, $s_2^* = s_2 / s_w$, $\sigma = S_y / S_s b$, $\kappa = K_z / K_r$, $\rho = r / r_w$, $\rho_w = r_w / b$, $\alpha_w = \kappa \rho_w^2$, $\alpha = \alpha_w \rho^2$, $\tau = K_r t / S_s r_w^2$, $\zeta = z / b$, and $\zeta_l = z_l / b$ where s_1^* and s_2^* stand for the dimensionless drawdowns for regions 1 and 2, respectively, σ is the ratio between specific yield S_y and the storativity $S_s b$, κ represents the dimensionless conductivity ratio, ρ denotes the dimensionless radial distance, ρ_w is the dimensionless radius of the pumping well, τ refers to the dimensionless time during the test, ζ and ζ_l are the dimensionless vertical distance and the dimensionless distance from the bottom of

aquifer to the bottom of the screen, respectively.

Taking the Laplace transform to the dimensionless governing equations of Eqs. (A1) and (A2) subject to the dimensionless boundary conditions of Eqs. (A4) – (A11), the Laplace-domain solutions for the dimensionless drawdowns in regions 1 and 2 are respectively

$$\tilde{s}_1^*(\rho, \zeta, p) = \sum_{m=0}^{\infty} A_{1m}'(p) \frac{I_0(\sqrt{p + \omega_{1m}} \cdot \rho)}{I_0(\sqrt{p + \omega_{1m}})} \cos(\Omega_{1m} \zeta) \quad (14)$$

and

$$\tilde{s}_2^*(\rho, \zeta, p) = \sum_{n=0}^{\infty} A_{2n}'(p) \frac{K_0(\sqrt{p + \omega_{2n}} \cdot \rho)}{K_0(\sqrt{p + \omega_{2n}})} \cos(\Omega_{2n} \zeta) \quad (15)$$

Applying the continuity conditions to Eq. (14) and Eq. (15), the coefficient A_{1m}' and A_{2n}' are respectively obtained as

$$A_{1m}'(p) = -i_{om} \left[\frac{2\Omega_{1m}}{\sin(2\Omega_{1m}) + 2\Omega_{1m}} \right] \cdot \sum_{n=0}^{\infty} A_{2n}'(p) k_{0n} \left[\frac{\sin[(\Omega_{1m} + \Omega_{2n})\zeta_l]}{\Omega_{1m} + \Omega_{2n}} + \frac{\sin[(\Omega_{1m} - \Omega_{2n})\zeta_l]}{\Omega_{1m} - \Omega_{2n}} \right] \quad (16)$$

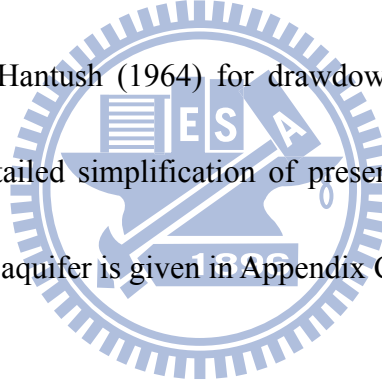
and

$$A_{2n}'(p) = \left[\frac{2\Omega_{2n}}{\sin(2\Omega_{2n}) + 2\Omega_{2n}} \right] \cdot \sum_{m=0}^{\infty} A_{1m}'(p) \left[\frac{\sin[(\Omega_{1m} + \Omega_{2n})\zeta_l]}{\Omega_{1m} + \Omega_{2n}} + \frac{\sin[(\Omega_{1m} - \Omega_{2n})\zeta_l]}{\Omega_{1m} - \Omega_{2n}} \right] + \frac{4}{p} \left[\frac{\sin(\Omega_{2n}) - \sin(\Omega_{2n}\zeta_l)}{\sin(2\Omega_{2n}) + 2\Omega_{2n}} \right] \quad (17)$$

where p is the Laplace variable and the symbols A_{1m}' , A_{2n}' , Ω_{1m} , Ω_{2n} , $I_0(\cdot)$, $I_1(\cdot)$, $K_0(\cdot)$, $K_1(\cdot)$, and k_0 are defined in Notation. The detailed derivations of Eqs. (14) and (15) are given in Appendix A.

2.3 Fully penetrating wells in unconfined and confined aquifers

Letting $\zeta_l = 0$ in Eqs. (16) and (17), the drawdown solution of Eq. (14) in region 1 is equal to zero and the Laplace-domain solution in Eq. (15) for dimensionless drawdown in region 2 with fully penetrating wells in unconfined aquifers is exactly the same as the solution given in Chen and Chang (2003, Eq. (7)) when the skin factor S_k equals to zero after some algebraic manipulations. The detailed derivation for reducing the present solution to the case of a fully penetrating well in unconfined aquifers is given in Appendix B. Furthermore, by setting $\zeta_l = 0$ and $\sigma = 0$, the Laplace-domain solution of Eq. (15) in region 2 can be reduced to the solution in Hantush (1964) for drawdown with a fully penetrating well in confined aquifers. The detailed simplification of present solution to the situation of fully penetrating well in confined aquifer is given in Appendix C.



CHAPTER 3 NUMERICAL EVALUATION

The numerical inversion given by Stehfest (1970) is adopted for calculating the time-domain drawdown solutions in Eqs. (14) and (15) for regions 1 and 2, respectively. Since there might be a problem of slow convergence when evaluating the infinite sums in Eqs. (14) and (15), the Shanks method is applied to accelerate convergence for these infinite sums.

3.1 Shanks Method

The Shanks method, also called the ε -algorithm, is a non-linear sequence-to-sequence transformation. Shanks (1955) proved that this transformation is effective when applied to accelerate the convergence of some slowly convergent sequences.

The partial sums, S_n , of an infinite series may be defined as

$$S_n = \sum_{k=0}^n a_k \quad (18)$$

where a_k is the k th term of the series. Based on the sequence of partial sums, the Shanks transform may be expressed as (Wynn, 1956)

$$e_{i+1}(S_n) = e_{i-1}(S_{n+1}) + \frac{1}{e_i(S_{n+1}) - e_i(S_n)}, \quad i = 1, 2, \dots \quad (19)$$

where $e_0(S_n) = S_n$ and $e_1(S_n) = [e_0(S_{n+1}) - e_0(S_n)]^{-1}$.

It is necessary to set a certain convergence criterion when applying the Shanks transform to evaluate a given series. Therefore, one defines a convergence factor, ERR, as

$$|e_{2i+2}(S_{n-1}) - e_{2i}(S_n)| \leq ERR \quad (20)$$

The sequence of partial sums is terminated when this criterion is met and the infinite series converges to the calculated $e_{2i+2}(S_{n-1})$.

This method has been successfully applied to compute the solutions arisen in the groundwater area (see, e.g., Yang and Yeh, 2002; Peng et al., 2002).

3.2 Numerical Inversion

The Laplace transform method is used to solve differential equations along with their corresponding initial and boundary conditions. In many engineering problems, the Laplace-domain solutions for mathematical models are tractable, yet the corresponding solutions in the time domain may not be possibly or easily solved. Under such circumstances, the methods of numerical Laplace inversion such as Stehfest algorithm (Stehfest, 1970) or the Crump algorithm (Crump, 1976) may be used.

The Laplace transform of a real-valued function $f(t)$, $t \geq 0$, is define as

$$F(p) = \int_0^{\infty} e^{-pt} f(t) dt \quad (21)$$

And the inverse of $F(p)$ is given by

$$f(t) = \frac{1}{2\pi i} \int_{\xi-\infty}^{\xi+\infty} e^{pt} F(p) dp \quad (22)$$

where ξ is in the region of any singularities of $F(p)$.

Stehfest (1970) presented algorithm for the numerical inversion of a Laplace-domain

expression. If $F(p)$ is the Laplace transform, then the inverse $f(t)$ can be approximately computed by

$$f(t) \approx \left[\frac{\ln(2)}{t} \right] \sum_{n=1}^N V_n F \left[\frac{n \cdot \ln(2)}{t} \right] \quad (23)$$

where the quantity $n \ln(2)/t$ substitutes the Laplace parameter p .

The coefficients V_n are given by

$$V_n = (-1)^{n+(N/2)} \sum_{k=(n+1)/2}^{\min(n, N/2)} \frac{k^{N/2} (2k)!}{(N/2 - k)! k! (k-1)! (n-k)! (2k-n)!} \quad (24)$$

where N is an even number, k is the value of $\text{Floor}((n+1)/2)$ where the function $\text{Floor}(\cdot)$ maps a real number to the largest previous integer.

To use the Stehfest method, it is necessary to choose N , the number of terms to sum. Theoretically, the larger the value of N , the more accurate the numerical solution. In fact, N is limited by truncation errors. Thus, the use of large N values causes subtraction of one large number from another, with a resulting loss of accuracy. Cheng and Siduruk (1994) suggest the range $6 \leq N \leq 20$. This study uses $N=8$ in computing the solutions, which can obtain accurate results. Note that the use of fewer or more terms of N may create inaccurate result.

CHAPTER 4 RESULTS AND DISCUSSION

4.1 Effective distance for the observation well with different specific time

Figure 2a demonstrates the dimensionless drawdown distributions for the dimensionless distance $\rho = 1, 1.1$ and 1.5 at the dimensionless time $\tau = 1$, while Figure 2b for $\rho = 1, 2$, and 5 at $\tau = 10^2$, Figure 2c for $\rho = 1, 2$ and 7 at $\tau = 10^4$, and Figure 2d for $\rho = 1, 5$ and 7 at $\tau = 10^6$. The aquifer parameters used in these figures are as follows: $\beta = 100$, $\kappa = 1$, $S = S_s b = 10^{-4}$, $S_y = 0.1$ and $\zeta_l = 0.5$. These figures show that the dimensionless drawdown at $\rho = 1$ match the boundary condition of the wellbore at different time periods. The dimensionless drawdown decreases with increasing ρ at $\tau = 1, 10^2, 10^4$ and 10^6 . In addition, it is apparent that vertical flows occur at the water table due to the free surface boundary as shown in Figures 2b – 2d.

4.2 Influence of specific yield

Figure 3 is plotted to examine the effect of specific yield S_y of region 2 on the dimensionless drawdown during CHT. This figure shows the response of dimensionless drawdown in a 100 m thick aquifer at $\rho = 50$, $\kappa = 1$, $S = 10^{-4}$, $\zeta = 0.75$ and $\zeta_l = 0.5$ for S_y ranging from 0 to 0.3. The dimensionless drawdown decreases with increasing S_y . The typical three-stage drawdown patterns can be observed. The water releases from the

elastic behavior of the aquifer formation at early time, i.e., the first stage. During the second stage at the moderate times, the gravity drainage almost stabilizes the water table. Finally, the effect of vertical flow vanishes at late times and the flow acts like Theis behavior again. Figure 3 shows that the larger S_y is, the longer delayed yield stage will be. The reason might be that larger S_y supply more water from the drainage. If $S_y = 0$, the top boundary represented by Eq. (7) becomes the no-flow condition and the aquifer can therefore be considered as confined condition.

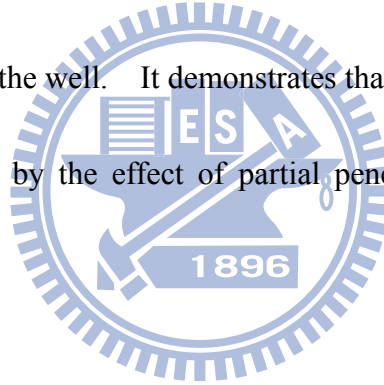
4.3 Effect of screen length

Figure 4 illustrates the distributions of the dimensionless drawdown at the well screen extends from $\zeta = \zeta_l$ to $\zeta = \beta$ in region 2 when $\tau = 10^6$. This figure shows the dimensionless drawdown increases with the length of well screen. The lines illustrate the positions of the well bottom for different length of well screen. In addition, it can be observed from the figure that large slopes of the drawdown distribution curves occur near the free surface boundary and the edge of the screen. Therefore, vertical groundwater flows are obviously large at these two areas.

4.4 Effective distance for the observation well

The response of dimensionless drawdown versus dimensionless time at different

observed location is plotted in Figure 5 for $\rho = 10$ and 100 with $\beta = 100$, $\kappa = 1$, $S = 10^{-4}$ and $\zeta_l = 0.25$. The S_y is zero for confined aquifer and there is no vertical flow as shown in Figure 5(a). On the other hand, the vertical flow is apparent at moderate times for different radial distances as demonstrated in Figure 5(b) when $S_y = 0.1$. Figures 6(a) and 6(b) illustrates the spatial flow pattern for $S_y = 0$ and 0.1 at $\tau = 10^4$ with the same parameter values as those to draw Figure 5. Apparently, the vertical flow occurs only near the bottom edge of the well screen when the aquifer is confined. However, for unconfined aquifers, the flow at free surface is almost vertical and obvious vertical flows occur near both the top and bottom edges of the well. It demonstrates that the vertical flow in the unconfined system is induced not only by the effect of partial penetration but also the effect of free surface boundary.



4.5 Effect of anisotropy

Figure 7 demonstrates the effect of the conductivity ratio $\kappa (= K_z / K_r)$ on the dimensionless drawdown during CHT. The vertical axis represents the dimensionless drawdown and the horizontal axis represents the dimensionless time. The κ ranges from 10^{-2} to 1 with $K_r = 10^{-4}$ m/min, $\beta = 100$, $S = 10^{-4}$, $S_y = 0.1$, and $\zeta_l = 0.5$. The dimensionless drawdown decreases with increasing κ indicating that the vertical flow from delayed gravity drainage becomes large for greater κ .

4.6 Influence of the well radius

Figure 8 illustrates the effect of the well radius on drawdown distribution in a 10 m thick aquifer. The considered well radii are 1, 0.1 and 0.01 m with $\sigma = 10^3$, $\zeta = 0.75$, $\zeta_l = 0.5$ and $\kappa = 1$. Drawdown is calculated at the distances of 3.16, 10, or 31.6 m from the pumping well for $\alpha = 10^{-1}$, 1, and 10^1 , respectively. The drawdown decreases with increasing distance from pumping well for different r_w as demonstrated in Figures 2a-d. The drawdown increases with r_w for different value of α , indicating that the well radius has significant effect on the drawdown distribution.

4.7 Effect of partially penetration

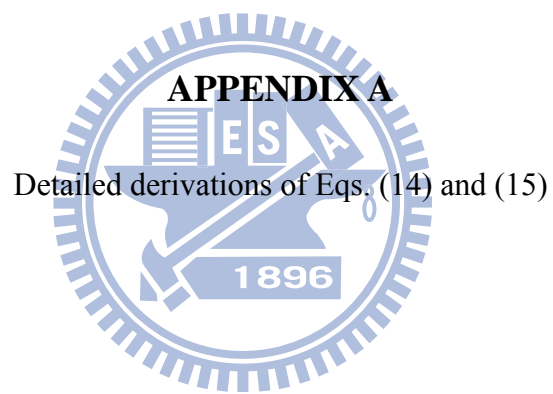
The effect of α on drawdown in the aquifer at $\zeta = 0$ when the well is fully ($\zeta_l = 0$) and partially penetrating ($\zeta_l = 0.8$), is plotted in Figure 9 for $\sigma = 10^3$ and $\kappa = 1$. The drawdown difference between the cases of full penetration and partial penetration decreases with increasing α . It is reasonable that $\alpha^{1/2}$ is directly proportional to the radial distance from the pumping well when the aquifer is isotropic and the partial penetration effect vanishes when the radial distance goes large. Since $r = \alpha^{1/2}b/\sqrt{\kappa}$, it is proved that the radial distance influenced by the partial penetration in unconfined aquifer under CHT is proportional to the aquifer thickness as well as the results from Hantush for confined aquifer under CFT.

CHAPTER 5 CONCLUSIONS

A semi-analytical solution of the drawdown distribution is developed for CHT performed in an unconfined aquifer with a partially penetrating well. The Laplace transforms and the method of separation of variables are employed to derive the transient drawdown in the Laplace domain for CHT. The Stehfest method is used to invert the solutions in time-domain and the Shanks method is applied to accelerate convergence in evaluating the infinite summations in the solution.

Large slopes of the drawdown distribution curves can be observed near the free surface boundary and the edge of the screen, which indicates that the vertical groundwater flows occur at these two areas. The dimensionless drawdown decreases with increasing S_y but increases with the length of well screen. For different r_w , the drawdown decreases with the increase of radial distance from pumping well and it might produce large error in drawdown if assuming the radius of pumping well is infinitesimal.

The present solution can be used for describing the transient drawdown distribution or investigating the effects of specific yield and conductivity ratio on the drawdown distribution in unconfined aquifers. In addition, the present solution can reduce to the solution for a fully penetrating well in either confined or unconfined aquifers under CHT.



APPENDIX A

Detailed derivations of Eqs. (14) and (15)

The dimensionless governing equations of Eqs. (1) and (3) can be expressed as

$$\frac{\partial^2 s_1^*}{\partial \rho^2} + \frac{1}{\rho} \frac{\partial s_1^*}{\partial \rho} + \alpha_w \frac{\partial^2 s_1^*}{\partial \zeta^2} = \frac{\partial s_1^*}{\partial \tau}, \quad 0 \leq \rho \leq 1, \quad 0 \leq \zeta \leq \zeta_l \quad (\text{A1})$$

and

$$\frac{\partial^2 s_2^*}{\partial \rho^2} + \frac{1}{\rho} \frac{\partial s_2^*}{\partial \rho} + \alpha_w \frac{\partial^2 s_2^*}{\partial \zeta^2} = \frac{\partial s_2^*}{\partial \tau}, \quad 1 \leq \rho < \infty, \quad 0 \leq \zeta \leq 1 \quad (\text{A2})$$

The dimensionless initial conditions for regions 1 and 2 are

$$s_1^*(\rho, \zeta, 0) = s_2^*(\rho, \zeta, 0) = 0 \quad (\text{A3})$$

and the boundary conditions at the bottom and top of the aquifer for regions 1 and 2 in terms

of dimensionless form can be written as

$$\left. \frac{\partial s_1^*(\rho, \zeta, \tau)}{\partial \zeta} \right|_{\zeta=0} = \left. \frac{\partial s_2^*(\rho, \zeta, \tau)}{\partial \zeta} \right|_{\zeta=0} = 0 \quad (\text{A4})$$

$$\left. \frac{\partial s_1^*(\rho, \zeta, \tau)}{\partial \zeta} \right|_{\zeta=\zeta_l} = 0, \quad 0 \leq \rho \leq 1 \quad (\text{A5})$$

and

$$\left. \frac{\partial s_2^*(\rho, \zeta, \tau)}{\partial \zeta} \right|_{\zeta=1} = - \left. \frac{\sigma}{\alpha_w} \frac{\partial s_2^*(\rho, \zeta, \tau)}{\partial \tau} \right|_{\zeta=1}, \quad 1 \leq \rho < \infty \quad (\text{A6})$$

The dimensionless boundary conditions at $\rho = 0$ and infinity are respectively written as

$$\frac{\partial s_1^*(0, \zeta, \tau)}{\partial \rho} = 0, \quad 0 < \zeta < \zeta_l \quad (\text{A7})$$

$$s_2^*(\infty, \zeta, \tau) = 0 \quad (\text{A8})$$

The dimensionless boundary condition along the screen is expressed as

$$s_2^*(1, \zeta, \tau) = 1, \quad \zeta_l < \zeta < 1, \quad \tau > 0 \quad (\text{A9})$$

In dimensionless form, continuity conditions become

$$s_1^*(1, \zeta, \tau) = s_2^*(1, \zeta, \tau), \quad 0 < \zeta < \zeta_l, \quad \tau > 0 \quad (\text{A10})$$

and

$$\left. \frac{\partial s_1^*(\rho, \zeta, \tau)}{\partial \rho} \right|_{\rho=1} = \left. \frac{\partial s_2^*(\rho, \zeta, \tau)}{\partial \rho} \right|_{\rho=1}, \quad 0 < \zeta < \zeta_l, \quad \tau > 0 \quad (\text{A11})$$

The Laplace transform is defined as:

$$\tilde{s}_1^*(\rho, \zeta, p) = L_p[s_1^*(\rho, \zeta, \tau); \tau \rightarrow p] = \int_0^\infty s_1^*(\rho, \zeta, \tau) e^{-p\tau} d\tau \quad (\text{A12})$$

where $\tilde{s}_1^*(\rho, \zeta, p)$ is the dimensionless drawdown in Laplace domain. The solution for the

dimensionless drawdown solutions can be obtained by taking Laplace transforms of

governing equations Eqs. (A1) to (A2) using the initial condition (A3) and the results are

$$\frac{\partial^2 \tilde{s}_1^*}{\partial \rho^2} + \frac{1}{\rho} \frac{\partial \tilde{s}_1^*}{\partial \rho} + \alpha_w \frac{\partial^2 \tilde{s}_1^*}{\partial \zeta^2} = p \tilde{s}_1^*, \quad 0 \leq \rho \leq 1, \quad 0 \leq \zeta \leq \zeta_l \quad (\text{A13})$$

and

$$\frac{\partial^2 \tilde{s}_2^*}{\partial \rho^2} + \frac{1}{\rho} \frac{\partial \tilde{s}_2^*}{\partial \rho} + \alpha_w \frac{\partial^2 \tilde{s}_2^*}{\partial \zeta^2} = p \tilde{s}_2^*, \quad 1 \leq \rho < \infty, \quad 0 \leq \zeta \leq 1 \quad (\text{A14})$$

The transformed boundary conditions at the bottom and top of the aquifer for regions 1 and 2

can be written as

$$\left. \frac{\partial \tilde{s}_1^*(\rho, \zeta, p)}{\partial \zeta} \right|_{\zeta=0} = \left. \frac{\partial \tilde{s}_2^*(\rho, \zeta, p)}{\partial \zeta} \right|_{\zeta=0} = 0 \quad (\text{A15})$$

$$\left. \frac{\partial \tilde{s}_1^*(\rho, \zeta, p)}{\partial \zeta} \right|_{\zeta=\zeta_l} = 0, \quad 0 < \rho < 1 \quad (\text{A16})$$

and

$$\left. \frac{\partial \tilde{s}_2^*(\rho, \zeta, p)}{\partial \zeta} \right|_{\zeta=1} = -\frac{\sigma}{\alpha_w} \cdot p \cdot \tilde{s}_2^*(\rho, \zeta=1, p) \quad (\text{A17})$$

In the same fashion, the transformed boundary conditions at $\rho = 0$ and ∞ are

$$\frac{\partial \tilde{s}_1^*(0, \zeta, p)}{\partial \rho} = 0, \quad 0 < \zeta < \zeta_l \quad (\text{A18})$$

and

$$\tilde{s}_2^*(\infty, \zeta, p) = 0 \quad (\text{A19})$$

After taking the Laplace transform, the boundary condition along the well screen is

$$\tilde{s}_2^*(1, \zeta, p) = \frac{1}{p}, \quad \zeta_l < \zeta < 1, \quad \tau > 0 \quad (\text{A20})$$

and continuity conditions become

$$\tilde{s}_1^*(1, \zeta, p) = \tilde{s}_2^*(1, \zeta, p), \quad 0 < \zeta < \zeta_l \quad (\text{A21})$$

and

$$\left. \frac{\partial \tilde{s}_1^*(\rho, \zeta, p)}{\partial \rho} \right|_{\rho=1} = \left. \frac{\partial \tilde{s}_2^*(\rho, \zeta, p)}{\partial \rho} \right|_{\rho=1}, \quad 0 < \zeta < \zeta_l \quad (\text{A22})$$

Assume that \tilde{s}_1^* and \tilde{s}_2^* are the product of two distinct functions, i.e.,

$$\tilde{s}_1^*(\rho, \zeta, p) = F_1(\rho, p)G_1(\zeta, p) \quad \text{and} \quad \tilde{s}_2^*(\rho, \zeta, p) = F_2(\rho, p)G_2(\zeta, p), \quad \text{respectively.}$$

Equations (A13) and (A14) can be, respectively, transformed as

$$G_1 \frac{\partial^2 F_1}{\partial \rho^2} + G_1 \frac{1}{\rho} \frac{\partial F_1}{\partial \rho} + \alpha_w F_1 \frac{\partial^2 G_1}{\partial \zeta^2} = p F_1 G_1 \quad (\text{A23})$$

and

$$G_2 \frac{\partial^2 F_2}{\partial \rho^2} + G_2 \frac{1}{\rho} \frac{\partial F_2}{\partial \rho} + \alpha_w F_2 \frac{\partial^2 G_2}{\partial \zeta^2} = p F_2 G_2 \quad (\text{A24})$$

Dividing throughout Equations (A23) and (A24) by $F_1 G_1$ and $F_2 G_2$, respectively, Equations

(A23) and (A24) can then be separated into the following two systems of ordinary differential

equations after some arrangements

$$\frac{\partial^2 G_1}{\partial \zeta^2} + \frac{\omega_{1m}}{\alpha_w} G_1 = 0 \quad (\text{A25})$$

$$\frac{\partial^2 F_1}{\partial \rho^2} + \frac{1}{\rho} \frac{\partial F_1}{\partial \rho} - [p + \omega_{1m}] F_1 = 0 \quad (\text{A26})$$

and

$$\frac{\partial^2 G_2}{\partial \zeta^2} + \frac{\omega_{2n}}{\alpha_w} G_2 = 0 \quad (\text{A27})$$

$$\frac{\partial^2 F_2}{\partial \rho^2} + \frac{1}{\rho} \frac{\partial F_2}{\partial \rho} - [p + \omega_{2n}] F_2 = 0 \quad (\text{A28})$$

where ω_{1m} and ω_{2n} are separation constants.

The solutions of (A25) and (A27) subject to the boundary in (A15) are respectively

$$G_1(\zeta, p) = a_{1m}(p) \cos(\Omega_{1m} \zeta) \quad (\text{A29})$$

and

$$G_2(\zeta, p) = a_{2n}(p) \cos(\Omega_{2n} \zeta) \quad (\text{A30})$$

where $\Omega_{1m} = \sqrt{\omega_{1m} / \alpha_w}$ and $\Omega_{2n} = \sqrt{\omega_{2n} / \alpha_w}$, $a_{1m}(p)$ and $a_{2n}(p)$ are constants with respect to p . In addition, substituting (A29) into (A16) yields the following equation

$$\sin(\Omega_{1m} \zeta_l) = 0 \quad (\text{A31})$$

The eigenvalues Ω_{1m} in Equation (A29) can then determined by solving Equation (A31) and

the result is

$$\Omega_{1m} = \frac{m\pi}{\zeta_l}, \quad m = 0, 1, 2, \dots \quad (\text{A32})$$

Similarly, substituting (A30) into (A17) gives the following equation

$$\Omega_{2n} \sin(\Omega_{2n}) = \frac{\sigma}{\alpha_w} p \cos(\Omega_{2n}), \quad n = 0, 1, 2, \dots \quad (\text{A33})$$

Equation (A33) can be numerically solved to obtain the eigenvalues Ω_{2n} in Equation (A30).

The general solutions of (A26) and (A28) are respectively

$$F_1(\rho, p) = c_{1m}(p)I_0(\sqrt{p + \omega_{1m}\rho}) + d_{1m}(p)K_0(\sqrt{p + \omega_{1m}\rho}) \quad (\text{A34})$$

and

$$F_2(\rho, p) = c_{2n}(p)I_0(\sqrt{p + \omega_{2n}\rho}) + d_{2n}(p)K_0(\sqrt{p + \omega_{2n}\rho}) \quad (\text{A35})$$

where $c_{1m}(p)$, $d_{1m}(p)$, $c_{2n}(p)$ and $d_{2n}(p)$ are constants.

Then, substituting (A34) into (A18) and (A35) into (A19), respectively, yields

$$\left. \frac{\partial F_1(\rho, p)}{\partial \rho} \right|_{\rho=0} = c_{1m}(p)I_1(0) - d_{1m}(p)K_1(0) \quad (\text{A36})$$

and

$$F_2(\infty, p) = c_{2n}(p)I_0(\infty) + d_{2n}(p)K_0(\infty) \quad (\text{A37})$$

where $c_{1m}(p)$ and $d_{2n}(p)$ are constants. Note that $d_{1m}(p)$ and $c_{2n}(p)$ equal zero because $K_1(0)$ and $I_0(\infty)$ are, respectively, equal to infinity.

The solutions of (A26) and (A28) are respectively

$$F_1(\rho, p) = c_{1m}(p)I_0(\sqrt{p + \omega_{1m}\rho}) \quad (\text{A38})$$

and

$$F_2(\rho, p) = d_{2n}(p)K_0(\sqrt{p + \omega_{2n}\rho}) \quad (\text{A39})$$

The product of (A29) and (A38) gives the general solution of Equation (A23) as

$$\tilde{s}_{1m}^*(\rho, \zeta, p) = A_{1m}(p)I_0(\sqrt{p + \omega_{1m}\rho}) \cos(\Omega_{1m}\zeta) \quad m = 0, 1, 2, \dots \quad (\text{A40})$$

where $A_{1m}(p)$ equals the product of $a_{1m}(p)$ and $c_{1m}(p)$. On the other hand, the product of (A30) and (A39) forms the general solution of Equation (A24) as

$$\tilde{s}_{2n}^*(\rho, \zeta, p) = A_{2n}(p)K_0(\sqrt{p + \omega_{2n}}\rho) \cos(\Omega_{2n}\zeta) \quad n = 0, 1, 2, \dots \quad (\text{A41})$$

where $A_{2n}(p)$ is the product of $a_{2n}(p)$ and $d_{2n}(p)$. Accordingly, the linear combination of

all the m 's solutions yields the complete solution for $\tilde{s}_1^*(\rho, \zeta, p)$

$$\tilde{s}_1^*(\rho, \zeta, p) = \sum_{m=0}^{\infty} A_{1m}(p)I_0(\sqrt{p + \omega_{1m}}\rho) \cos(\Omega_{1m}\zeta) \quad (\text{A42})$$

Similarly, the complete solution for $\tilde{s}_2^*(\rho, \zeta, p)$ can be obtained as

$$\tilde{s}_2^*(\rho, \zeta, p) = \sum_{n=0}^{\infty} A_{2n}(p)K_0(\sqrt{p + \omega_{2n}}\rho) \cos(\Omega_{2n}\zeta) \quad (\text{A43})$$

The coefficients $A_{1m}(p)$ and $A_{2n}(p)$ are unknowns at this stage and can be solved from the

following equation obtained by substituting (A42) and (A43) into (A21) and (A20),

respectively, as

$$\sum_{n=0}^{\infty} A_{2n}(p)K_0(\sqrt{p + \omega_{2n}}) \cos(\Omega_{2n}\zeta) = \frac{1}{p}, \quad \zeta_l < \zeta < 1 \quad (\text{A44})$$

and

$$\sum_{m=0}^{\infty} A_{1m}(p)I_0(\sqrt{p + \omega_{1m}}) \cos(\Omega_{1m}\zeta) = \sum_{n=0}^{\infty} A_{2n}(p)K_0(\sqrt{p + \omega_{2n}}) \cos(\Omega_{2n}\zeta), \quad 0 < \zeta < \zeta_l \quad (\text{A45})$$

Equations (A40) and (A41) are organized and expressed as

$$\begin{aligned} \sum_{n=0}^{\infty} A_{2n}(p)K_0(\sqrt{p + \omega_{2n}}) \cos(\Omega_{2n}\zeta) &= \sum_{m=0}^{\infty} A_{1m}(p)I_0(\sqrt{p + \omega_{1m}}) \cos(\Omega_{1m}\zeta), \quad 0 < \zeta < \zeta_l \\ &= \frac{1}{p}, \quad \zeta_l < \zeta < 1 \end{aligned} \quad (\text{A46})$$

In order to obtain concise solutions, we further define $A_{2n}'(p) = A_{2n}(p)K_0(\sqrt{p + \omega_{2n}})$ and

$A_{1m}'(p) = A_{1m}(p)I_0(\sqrt{p + \omega_{1m}})$ and (A42) can be rewritten as

$$\sum_{n=0}^{\infty} A_{2n}'(p) \cos(\Omega_{2n}\zeta) = f(\zeta), \quad 0 < \zeta < 1 \quad (\text{A47})$$

where

$$\begin{aligned}
f(\zeta) &= \sum_{m=0}^{\infty} A_{1m}'(p) \cos(\Omega_{1m}\zeta), \quad 0 < \zeta < \zeta_l \\
&= \frac{1}{p}, \quad \zeta_l < \zeta < 1
\end{aligned} \tag{A48}$$

The term on the left-hand side (LHS) of Eq. (A47) is a half-range Fourier cosine series of the function on the right-hand side (RHS) of Eq. (A47) for the region $0 < \zeta < 1$. The coefficient $A_{2n}'(p)$ can then be obtained from the properties of Fourier series as

$$A_{2n}'(p) = \frac{\int_0^1 \cos(\Omega_{2n}\zeta) f(\zeta) d\zeta}{\int_0^1 \cos^2(\Omega_{2n}\zeta) d\zeta} \tag{A49}$$

Carrying out the integration in (A49) and simplifying the result yields the coefficient $A_{2n}'(p)$ as expressed in Eq. (17).

Similarly, substituting (A42) and (A43) into (A22), one can obtain

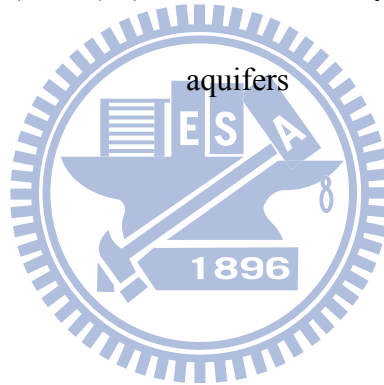
$$\sum_{m=0}^{\infty} A_{1m}'(p) \cos(\Omega_{1m}\zeta) = -\sum_{n=0}^{\infty} A_{2n}'(p) \sqrt{p + \omega_{2n}} \frac{K_1(\sqrt{p + \omega_{2n}})}{K_0(\sqrt{p + \omega_{2n}})} \cos(\Omega_{2n}\zeta), \quad 0 < \zeta < \zeta_l \tag{A50}$$

From (A50), the coefficient $A_{1m}'(p)$ can be determined as Equation (15).

Accordingly, based on the coefficients $A_{1m}'(p)$ and $A_{2n}'(p)$, the complete solution for \tilde{s}_1^* and \tilde{s}_2^* can be, respectively, obtained as Eqs. (14) and (15).

APPENDIX B

Simplification of Eqs. (15) and (16) to the case of fully penetrating well in unconfined



Letting $\zeta_l = 0$ in Eqs. (16) and (17), the drawdown solution of Eq. (14) in region 1 is equal to zero and the Laplace-domain solution in Eq. (15) for dimensionless drawdown in region 2 pumping from a fully penetrating well in unconfined aquifers can be expressed as

$$\tilde{s}_2^*(\rho, \zeta, p) = \sum_{n=0}^{\infty} \frac{4}{p} \left[\frac{\sin(\Omega_{2n})}{\sin(2\Omega_{2n}) + 2\Omega_{2n}} \right] \frac{K_0(\sqrt{p + \omega_{2n}} \cdot \rho)}{K_0(\sqrt{p + \omega_{2n}})} \cos(\Omega_{2n}\zeta) \quad (\text{B1})$$

Considering the skin effect in pumping system, Chen and Chang (2003) developed a Laplace-domain solution for describing the flow in an unconfined aquifer with pumping from a fully penetrating well under constant-head test. The solution is expressed as

$$h_D(\rho, \zeta, \tau) = L^{-1} \left\{ \frac{2}{p} \sum_{n=1}^{\infty} \frac{K_0(\chi_n \cdot \rho)}{K_0(\chi_n) + S_k \chi_n K_1(\chi_n)} \frac{\cos(\varepsilon_n \zeta)}{\lambda_n \cos(\varepsilon_n)} \right\} \quad (\text{B2})$$

$$\varepsilon \tan(\varepsilon) = \frac{\sigma p}{\beta} \quad (\text{B3})$$

$$\lambda = 1 + \sigma p / \beta + (\varepsilon_n^2 \beta / \sigma p) \quad (\text{B4})$$

where $\beta = (K_z / K_r)(r_w^2 / b^2)$, $\rho = r / r_w$, $\sigma = S_y / S$, $\chi_n = \sqrt{p + \beta \varepsilon_n^2}$, $\zeta = z / b$, $\tau = (Tt) / (r_w^2 S)$, ε_n is n th positive root of Eq. (B3), S_k is skin factor, p is Laplace transform parameter and $L^{-1}\{\}$ is the Laplace inversion operator.

If skin effect is negligible ($S_k = 0$), Eq. (B2) can be rearranged as

$$h_D(\rho, \zeta, \tau) = L^{-1} \left\{ \frac{2}{p} \sum_{n=1}^{\infty} \frac{K_0(\chi_n \cdot \rho)}{K_0(\chi_n)} \frac{\cos(\varepsilon_n \zeta)}{\lambda_n \cos(\varepsilon_n)} \right\} \quad (\text{B5})$$

Since Eqs. (B1) and (B5) are both used for calculating the dimensionless drawdown in unconfined aquifers with fully penetrating wells; these two equations should be identical. The mathematical derivation is provided in the following section to show that Eq. (B1) is exactly

identical to Eq. (B5).

Some definitions of variable in Eq. (B5) are different from that in Eq. (B1) and the relations are $\alpha_w = \beta$, $\Omega_{2n} = \varepsilon_n$ and $\sqrt{p + \omega_{2n}} = \chi_n$. Eq. (B5) can be thus rearranged as

$$h_D(\rho, \zeta, \tau) = L^{-1} \left\{ \frac{2}{p} \sum_{n=1}^{\infty} \frac{K_0(\sqrt{p + \omega_{2n}} \cdot \rho) \cos(\Omega_{2n} \zeta)}{K_0(\sqrt{p + \omega_{2n}}) \lambda_n \cos(\Omega_{2n})} \right\} \quad (\text{B6})$$

Substituting (B3) into Eq. (4), one can obtain

$$\lambda_n = 1 + \Omega_{2n} \tan(\Omega_{2n}) + \frac{\Omega_{2n}}{\tan(\Omega_{2n})} \quad (\text{B7})$$

In addition, substituting (B6) into the term on the left-hand side (LHS) of Eq. (B5) results in

$$\frac{1}{\lambda_n \cos(\Omega_{2n})} = \frac{1}{\left[1 + \Omega_{2n} \tan(\Omega_{2n}) + \frac{\Omega_{2n}}{\tan(\Omega_{2n})} \right] \cos(\Omega_{2n})} \quad (\text{B8})$$

Using the tangent relation (i.e., $\tan(\mathcal{G}) = \sin(\mathcal{G})/\cos(\mathcal{G})$), the denominator on the right-hand side (RHS) of Eq. (B8) can be expressed as

$$\frac{1}{\left[1 + \Omega_{2n} \tan(\Omega_{2n}) + \frac{\Omega_{2n}}{\tan(\Omega_{2n})} \right] \cos(\Omega_{2n})} = \frac{1}{\cos(\Omega_{2n}) + \Omega_{2n} \sin(\Omega_{2n}) + \frac{\Omega_{2n} \cos^2(\Omega_{2n})}{\sin(\Omega_{2n})}} \quad (\text{B9})$$

The RHS in Eq. (B8) can be further written as

$$\frac{1}{\cos(\Omega_{2n}) + \Omega_{2n} \sin(\Omega_{2n}) + \frac{\Omega_{2n} \cos^2(\Omega_{2n})}{\sin(\Omega_{2n})}} = \frac{1}{\cos(\Omega_{2n}) + \Omega_{2n} \left[\sin(\Omega_{2n}) + \frac{\cos^2(\Omega_{2n})}{\sin(\Omega_{2n})} \right]} \quad (\text{B10})$$

Eq. (B10) can be simplified using the triangle relationship (i.e., $\sin^2(\mathcal{G}) + \cos^2(\mathcal{G}) = 1$) as

$$\frac{1}{\cos(\Omega_{2n}) + \Omega_{2n} \left[\sin(\Omega_{2n}) + \frac{\cos^2(\Omega_{2n})}{\sin(\Omega_{2n})} \right]} = \frac{1}{\cos(\Omega_{2n}) + \frac{\Omega_{2n}}{\sin(\Omega_{2n})}} \quad (\text{B11})$$

By multiplying $\sin(\Omega_{2n})/\sin(\Omega_{2n})$, Eq. (B11) becomes

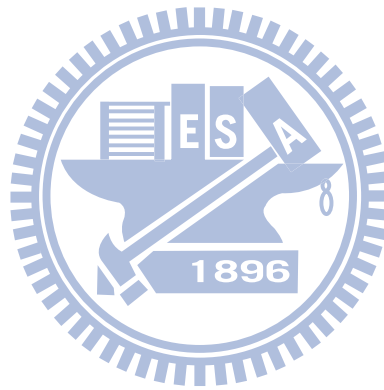
$$\frac{1}{\cos(\Omega_{2n}) + \frac{\Omega_{2n}}{\sin(\Omega_{2n})}} = \frac{2 \sin(\Omega_{2n})}{\sin(2\Omega_{2n}) + 2\Omega_{2n}} \quad (\text{B12})$$

From Eq. (B7) to (B11), the following relation is established

$$\frac{1}{\lambda_n \cos(\varepsilon_n)} = \frac{2 \sin(\Omega_{2n})}{\sin(2\Omega_{2n}) + 2\Omega_{2n}} \quad (\text{B13})$$

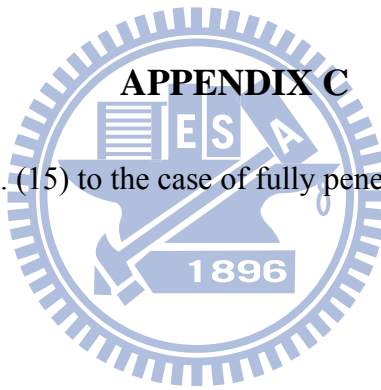
Furthermore, base on $\Omega_{2n} = \varepsilon_n$ and Eqs. (B6)-(B13), one can easily prove that Eq. (B1)

is identical to Eq. (B5).



APPENDIX C

Simplification of Eq. (15) to the case of fully penetrating wells in confined aquifer



The Laplace-domain solution of Eq. (15) in region 2 for describing the flow due to pumping from a fully penetrating well in confined aquifers can be expressed as

$$\tilde{s}_2^*(\rho, \zeta, p) = \sum_{n=0}^{\infty} \frac{4}{p} \left[\frac{\sin(\Omega_{2n})}{\sin(2\Omega_{2n}) + 2\Omega_{2n}} \right] \frac{K_0(\sqrt{p + \omega_{2n}} \cdot \rho)}{K_0(\sqrt{p + \omega_{2n}})} \cos(\Omega_{2n} \zeta) \quad (C1)$$

Substituting $\sigma = 0$ (i.e., $S_y = 0$ for confined aquifers) into Eq. (A33), one can obtain

$$\Omega_{2n} = n\pi \quad n = 0, 1, 2, \dots \quad (C2)$$

Substituting Eq. (C2) into Eq. (C1) and using L'Hospital's rule, Eq. (C1) is simplified as

$$\tilde{s}_2^*(\rho, \zeta, p) = \frac{1}{p} \frac{K_0(\sqrt{p} \cdot \rho)}{K_0(\sqrt{p})} \quad (C3)$$

The non-dimensional form of Eq. (C3) is

$$\frac{\tilde{s}_2(\rho, \zeta, p)}{s_w} = \frac{1}{p'} \frac{K_0\left(\sqrt{\frac{S_s r_w^2}{K_r}} p' \cdot \frac{r}{r_w}\right)}{K_0\left(\sqrt{\frac{S_s r_w^2}{K_r}} p'\right)} \quad (C4)$$

where $p' = (S_s r_w^2 / K_r) p$.

Eq. (C4) is further simplified as

$$\tilde{s}_2(\rho, \zeta, p) = s_w \frac{1}{p'} \frac{K_0\left(\sqrt{\frac{S_s}{K_r}} p' r\right)}{K_0\left(\sqrt{\frac{S_s}{K_r}} p' r_w\right)} \quad (C5)$$

Assuming the aquifer is confined, homogeneous and isotropic, the solution in Eq. (C5) is identical to the Laplace-domain solution in Hantush (1964) written as

$$\bar{s}(r, p) = s_w \cdot \frac{K_0(\lambda \cdot r)}{pK_0(\lambda \cdot r_w)} \quad (C6)$$

where $\lambda = \sqrt{(p \cdot S_s) / K}$.



REFERENCES

- Abdul, A. S. "A new pumping strategy for petroleum product recovery from contaminated hydrogeologic systems: Laboratory and field evaluations" *Ground Water Monit. Rem.* 12, pp.105-114, 1992.
- Batu, V. "Aquifer hydraulics: a comprehensive guide to hydrogeologic data analysis" *John Wiley & Sons Inc.*, New York, 1998.
- Boulton, N. S. "Unsteady radial flow to a pumped well allowing for delayed yield from storage" *Intern. Assoc. Sci. Hydrol., Rome. Pubi.*, 37, pp. 472-477, 1954.
- Chen, C. S., and Chang, C. C. "Well hydraulics theory and data analysis of the constant head test in an unconfined aquifer with the skin effect" *Water Resour. Res.*,39(5), pp. 1121-1135, 2003.
- Cheng, A. H.-D., and Siduruk, P. "Approximate Inversion of the Laplace Transform" *The Mathematic Journal*, 4 (2), pp.76-82, 1994.
- Crump, K.S., "Numerical inversion of Laplace trans- forms using a Fourier series approximation" *J. Assoc. Comput. Mach.*,23(1), pp. 89-96, 1976.
- Chang, Y. C., and Yeh, H. D. "New solutions to the constant-head test performed at a partially penetrating well" *J. Hydrology*, 369, pp. 90-97, 2009.
- Chang, Y. C., and Yeh, H. D. "A new analytical solution solved by triple series equations method for constant-head tests in confined aquifers" *Advances in Water Resources*, 33,

pp. 640-651, 2010.

Chang, Y. C., Yeh, H. D. and Chen, G. Y. "Transient solution for radial two-zone flow in unconfined aquifers under constant-head test" *Hydrological Processes*, 24, pp. 1496-1503, 2010.

Hantush, M.S. "Hydraulics of wells" in *Advances in Hydrosience*, vol. 1, V.T. Chow, eds., Academic. San Diego. Calif., pp. 281-432, 1964.

Hiller, C. K., and Levy, B. S. "Estimation of aquifer diffusivity from analysis of constant-head pumping test data" *Ground Water*, 32(1), pp. 47-52. 1994.

Javandel, I., Zaghi, N. "Analysis of flow to an extended fully penetrating well" *Water Resour. Res.*, 11(1), pp. 1059-164, 1975.

Jones, L., Lemar T., and Tsai, C. T. "Results of two pumping tests in Wisconsin age weathered till in Iowa" *Ground Water*, 30(4), pp. 529-538, 1992.

Jones, L. "A comparison of pumping and slug tests for estimating the hydraulic conductivity of unweathered Wisconsin age till in Iowa" *Ground Water*, 31(6), pp. 896-904, 1993.

Kirkham, D. "Exact theory of flow into a partially penetrating well" *J. Geophys. Res.*, 64(9), pp. 1317-1327, 1959.

Malama, B., Kuhlman, K.L., Barrash, W. "Semi-analytical solutions for flow in leaky unconfined aquifer-aquitard systems" *J. Hydrology*, 346(1-2), pp. 59-68, 2007.

Malama, B., Kuhlman, K.L., Barrash, W. "Semi-analytical solutions for flow in leaky

unconfined aquifer toward a partially penetrating pumping well” *J. Hydrology*, 356(1-2), pp. 234-244, 2008.

Malama, B., Kuhlman, K. L., Revil A. “A semi-analytical solution for transient streaming potentials associated with confined aquifer pumping tests” *Geophysical Journal International*, 176(3), pp. 1007-1016, 2009.

Malama, B., Kuhlman, K. L., Revil, A. “Theory of transient streaming potentials associated with axial-symmetric flow in unconfined aquifers” *Geophysical Journal International*, 179(2), pp.990-1003, 2009.

Mishra, S., and Guyonnet, D. “Analysis of observation-well response during constant-head testing” *Ground Water*, 30(4), pp. 523–528, 1992.

Moench, A. F. “Flow to a well of finite diameter in a homogeneous, anisotropic water table aquifer” *Water Resour. Res.*, 33(6), pp. 1397-1407, 1997.

Murdoch, L. D., and Franco, J. “The analysis of constant drawdown wells using instantaneous source functions” *Water Resour. Res.*, 30(1), pp. 117-127, 1994.

Neuman, S. P. “Theory of flow in unconfined aquifers considering delayed response of the water table” *Water Resour. Res.*, 8(4), pp. 1031-1045, 1972.

Neuman, S. P. “Effects of partial penetration on flow in unconfined aquifers considering delayed aquifer response” *Water Resour. Res.*, 10(2), pp. 303-312, 1974.

Pasandi, M., Samani, N., Barry, D.A. “Effect of wellbore storage and finite thickness skin on

flow to a partially penetrating well in a phreatic aquifer” *Adv. Water Resour.*, 31, pp. 383-398, 2008.

Peng, H. Y., Yeh, H. D. and Yang, S. Y. “Improved numerical evaluation of the radial groundwater flow equation” *Adv. Water Resour.*, 25(6), pp. 663-675, 2002.

Renard, P. “Approximate discharge for constant head test with recharging boundary” *Ground Water*, 43, pp. 439-442, 2005.

Rizzo, E., Suski, B., Revil, A., Straface, S., and Troisi, S. “Self-potential signals associated with pumping tests experiments” *Journal of Geophysical Research-Solid Earth*, 109(B10203), 2004.

Shanks, D. “Non-linear transformations of divergent and slowly convergent sequence” *J. Math. Phys.*, 34, pp. 1-42, 1955.

Singh SK. “Simple approximation of well function for constant drawdown variable discharge artesian wells” *J. Irrigation and Drainage Engineering* 133(3), pp. 282–285, 2007.

Stehfest, H. “Numerical inversion of Laplace transforms” *Comm. ACM* 13, pp. 47-49, 1970.

Theis, C.V. “The relation between the lowering of the piezometric surface and the rate and duration of discharge of a well using groundwater storage”, *Am. Geophys. Union Trans.*, 16, pp. 519-524, 1935.

Tartakovsky, G. D., and Neuman, S. P. “Three-dimensional saturated-unsaturated flow with axial symmetry to a partially penetrating well in a compressible unconfined aquifer”

Water Resour. Res., 43, W01410, doi:10.1029/2006WR005153, 2007.

Uraiet, A. A., and Raghavan, R. “Unsteady flow to a well producing at a constant pressure” *J.*

Pet. Technol., 32(10), pp. 1803-1812, 1980.

Yang, S. Y., and Yeh, H. D. “Solution for flow rates across the wellbore in a two-zone

confined aquifer” *J. Hydraul. Eng., ASCE*, 128(2), pp. 175-183, 2002.

Yang, S. Y., and Yeh, H. D. “Laplace-domain solutions for radial two-zone flow equations

under the conditions of constant-head and partially penetrating well” *J. Hydraul. Eng.,*

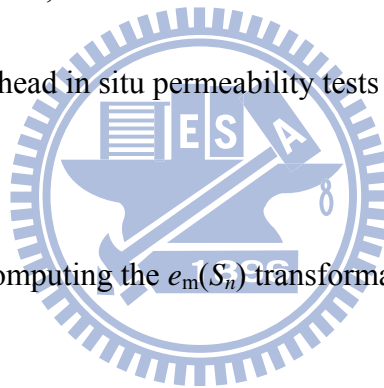
ASCE, 131(3), pp. 209-216, 2005.

Wilkinson, W. B. “Constant head in situ permeability tests in clay strata” *Geotechnique*, 18,

pp. 172-194, 1968.

Wynn, P. “On a device for computing the $e_m(S_n)$ transformation” *Math. Tables Aids Comput.*,

10, pp. 91-96, 1956.



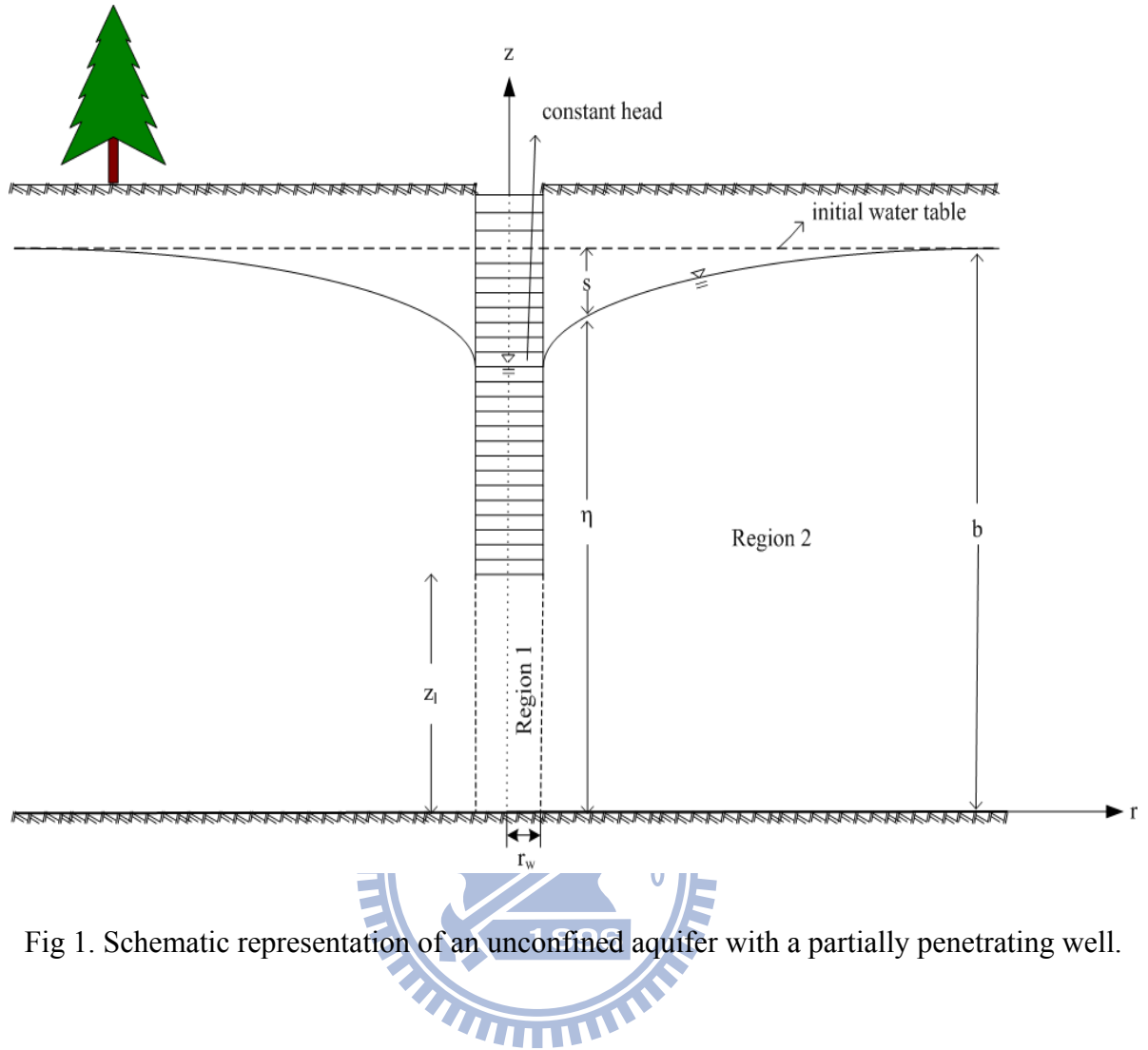


Fig 1. Schematic representation of an unconfined aquifer with a partially penetrating well.

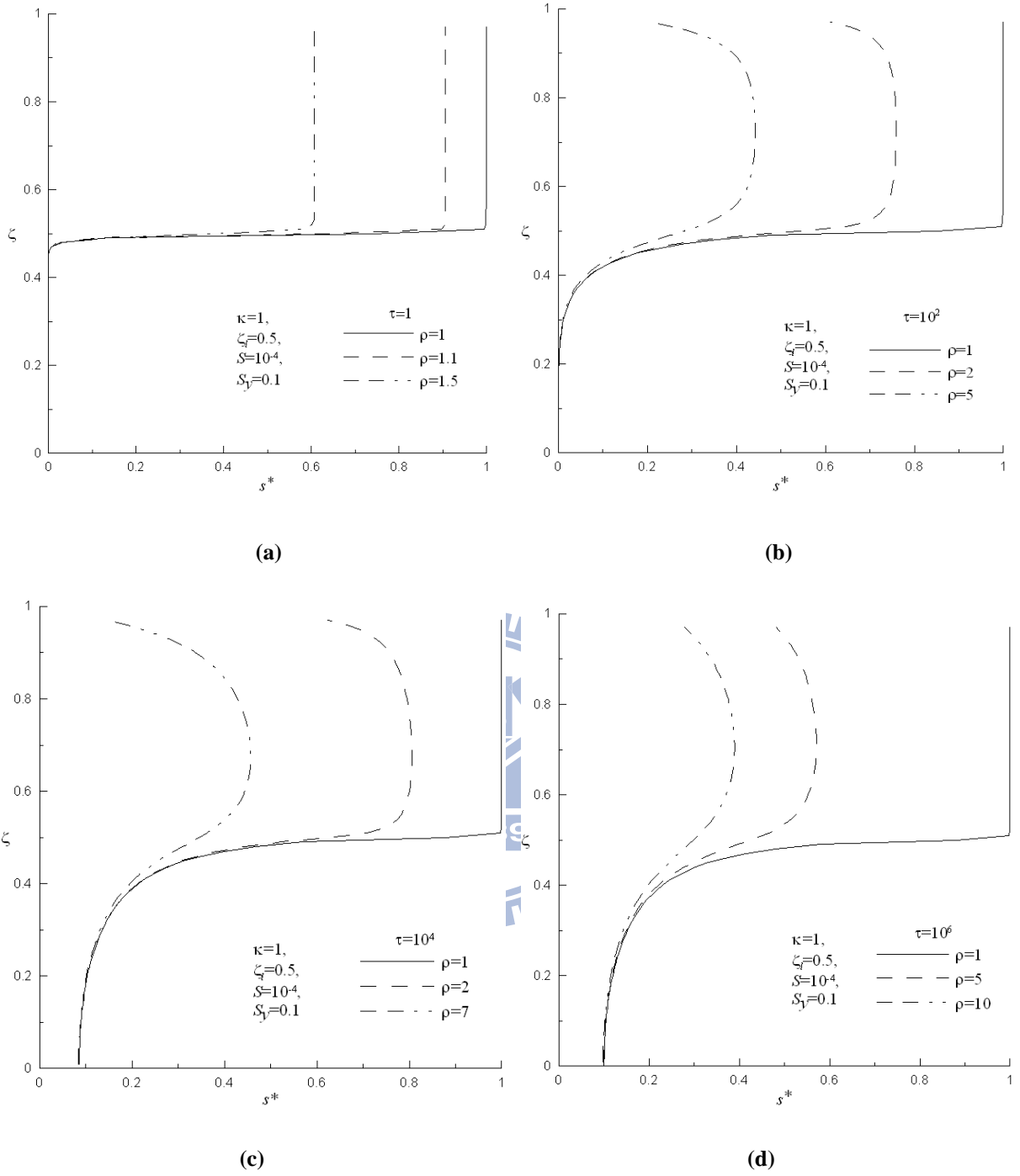


Fig 2. The dimensionless drawdown distributions at $\tau =$ (a) 1 , (b) 10^2 , (c) 10^4 , and (d)

10^6 .

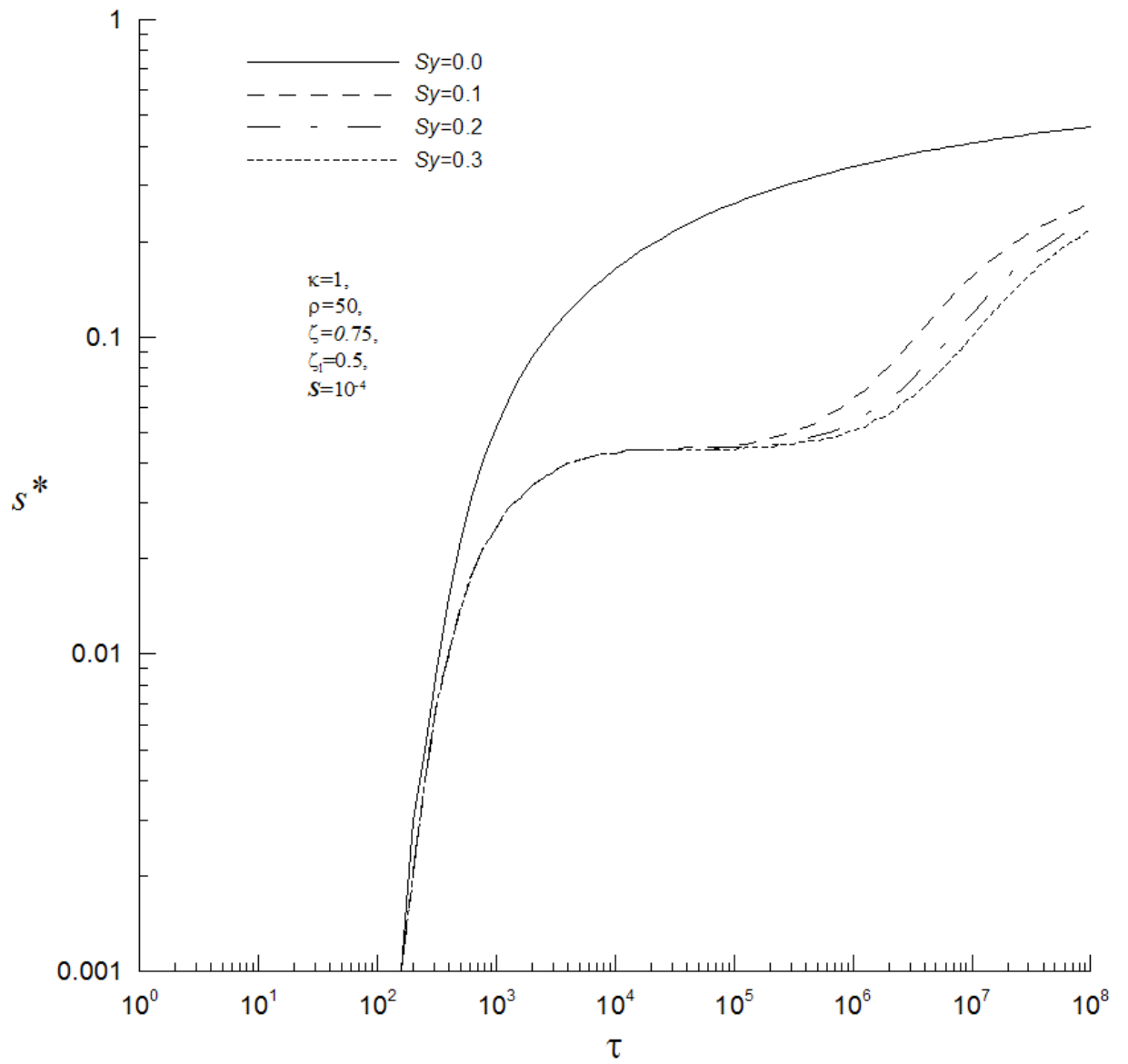


Fig 3. The effect of specific yield on the dimensionless drawdown during CHT.

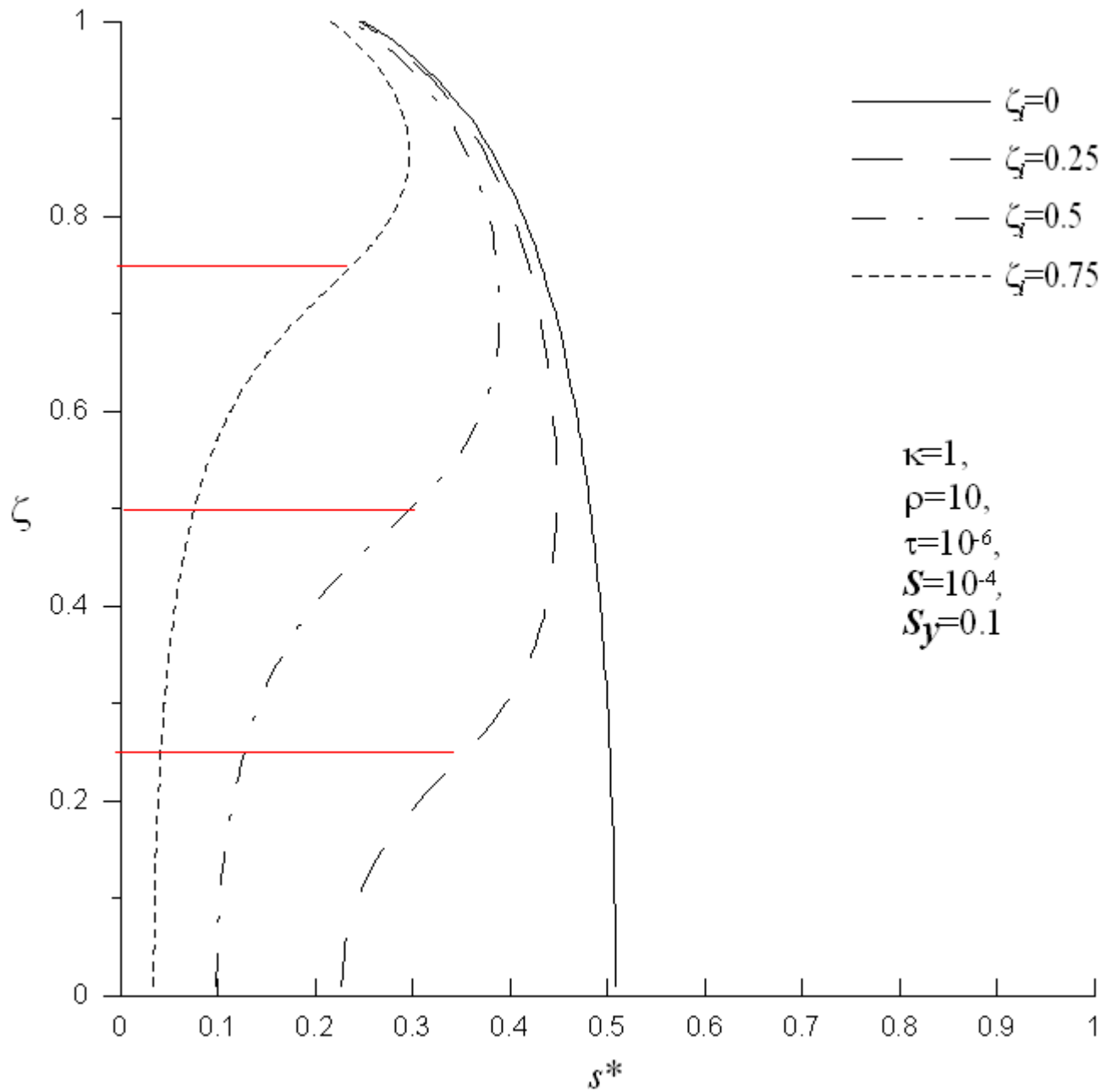
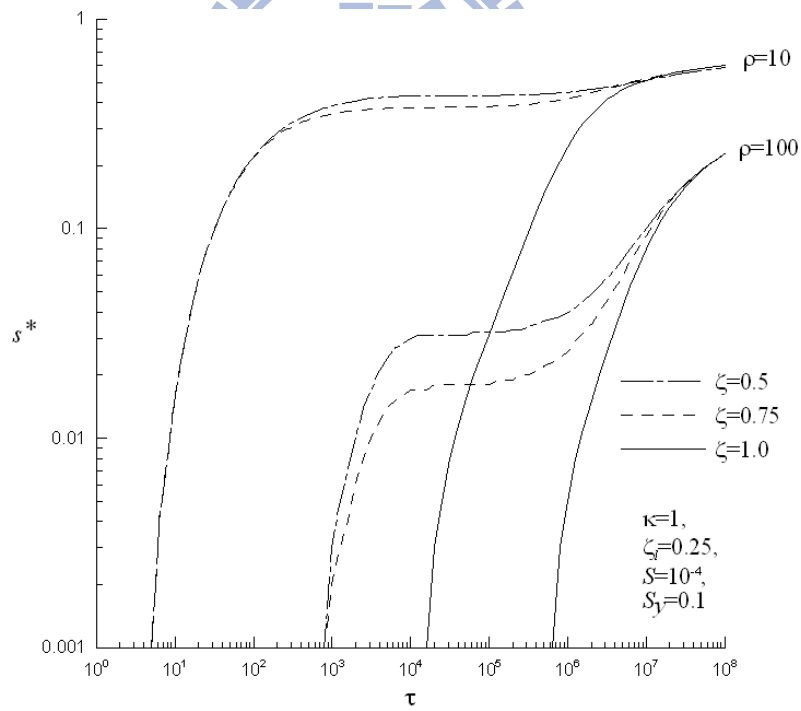
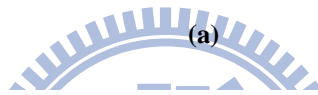
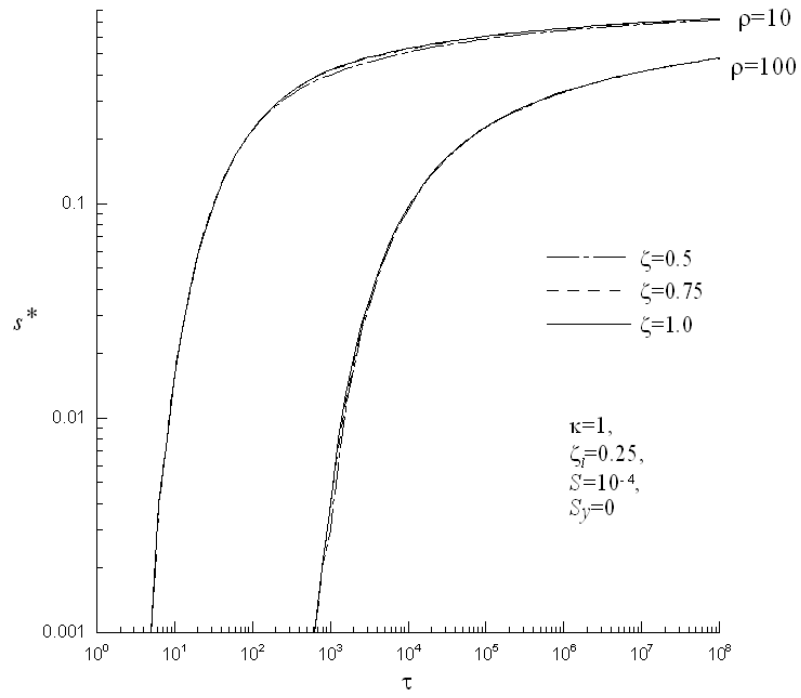
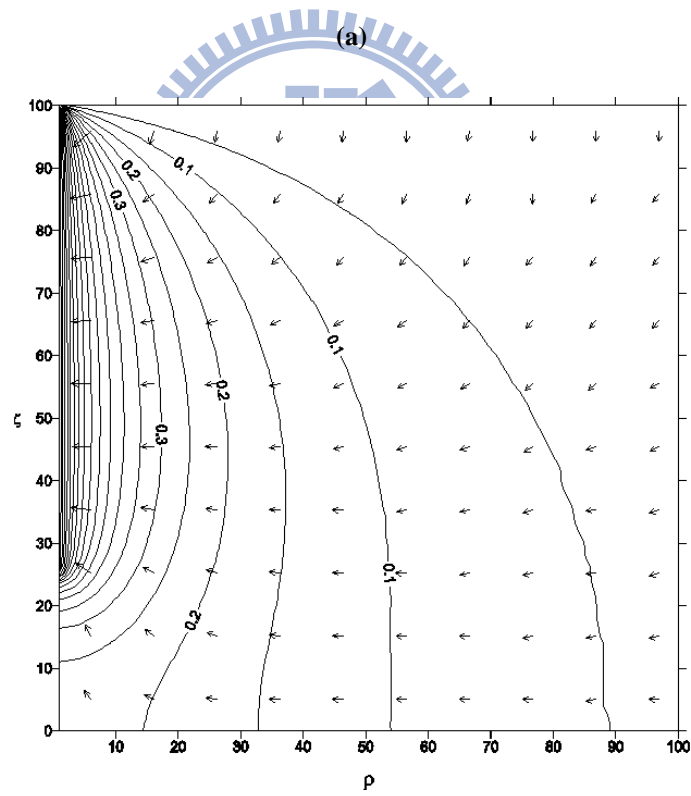
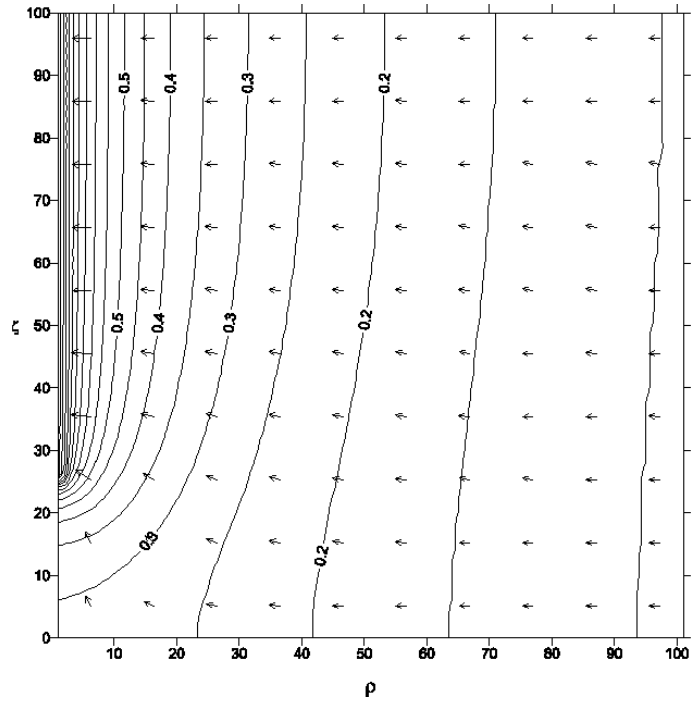


Fig 4. The dimensionless drawdown distributions at the well screen extended from $\zeta = \zeta_l$ to $\zeta = \beta$ in region 2.



(b)

Fig 5. Relationship for dimensionless drawdown versus dimensionless time with $\zeta = 50, 75,$ and 100 at $\rho = 10$ or 100 for $S_y =$ (a) 0 and (b) 0.1



(b)

Fig 6. Spatial flow pattern in an unconfined aquifer with a partially penetrating well for $\kappa = 1$,

$\beta = 100$, $\zeta_l = 25$, $S = 10^{-4}$ at $\tau = 10^4$ when $S_y =$ (a) 0 and (b) 0.1.

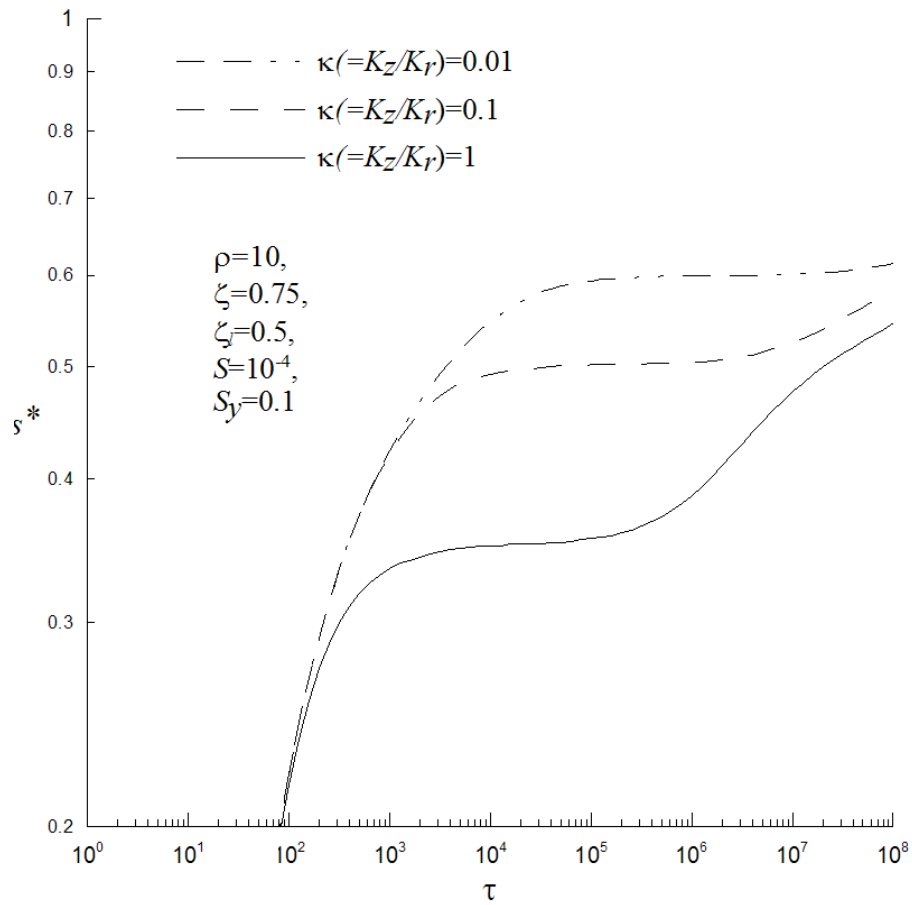


Fig 7. The effect of conductivity ratio (κ) of region 2 on the dimensionless drawdown during CHT.

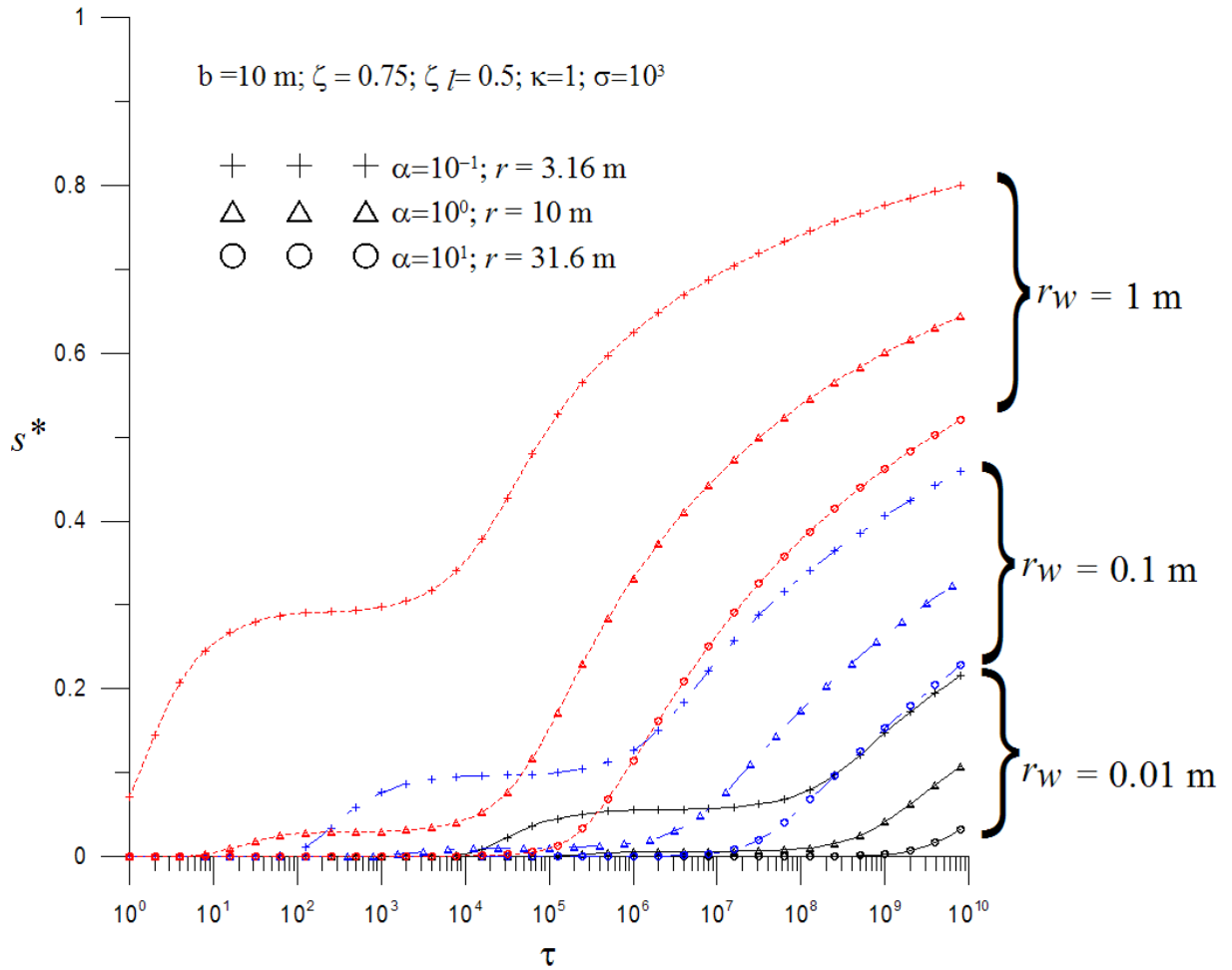


Fig 8. Drawdown distribution for a well with three different well radii ($r_w = 1, 0.1$ and 0.01 m)

with $\sigma = 10^3$, $\zeta = 0.75$, $\zeta_l = 0.5$ and $\kappa = 1$.

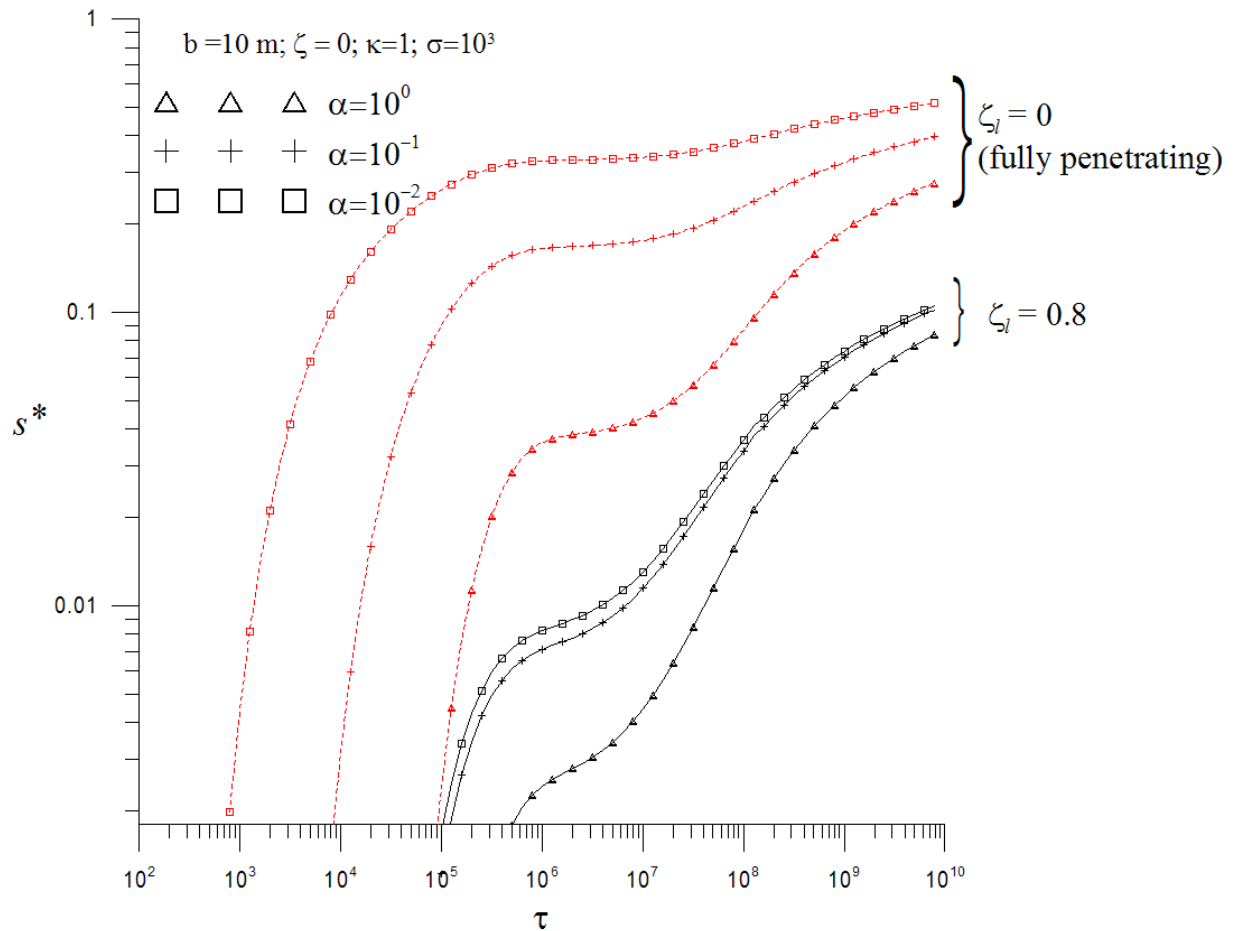


Fig 9. Effect of α on drawdown in a 100 m thick aquifer when $\sigma = 10^3$, $\kappa = 1$ at $\zeta = 0$ and $r = 100, 31.62$, and 10 m for $\alpha = 10^0, 10^{-1}$ and 10^{-2} , respectively.